



Jomo Kenyatta University of Agriculture and Technology
College of Engineering and Technology
School of Mechanical, Materials, and Manufacturing Engineering
Department of Mechatronic Engineering

Design and development of a cooling system for a liquid rocket engine

FYP 18-22

INTERIM REPORT

Michael Kimani (ENM221-0066/2017)

Felix Wanyoike Gateru (ENM221-0056/2017)

Supervisors

Dr. Shohei Aoki

Dr. Bernard Owiti

September, 2022

Submitted in partial fulfilment of the requirements for the degree of Bachelor of Science in Mechatronic Engineering in Jomo Kenyatta University of Agriculture and Technology, 2022.

Declaration

We hereby declare that the work contained in this report is original; researched and documented by the undersigned students. It has not been used or presented elsewhere in any form for award of any academic qualification or otherwise. Any material obtained from other parties have been duly acknowledged. We have ensured that no violation of copyright or intellectual property rights have been committed.

1. Michael Kimani

Signature..... Date.....

2. Felix Wanyoike Gateru

Signature..... Date.....

Approved by supervisors:

1. Dr. Shohei Aoki

Signature..... Date.....

2. Dr. Bernard Owiti

Signature..... Date.....

Abstract

Operation of rocket engines involve the generation of large amounts of heat during combustion. The thermal energy produced during propellant combustion is integral to rocket operation but can be detrimental to the structure of the rocket. There is therefore a need to cool the rocket body and protect it from heat damage. A number of techniques have been developed for cooling the chamber and the nozzle. These techniques have various advantages and disadvantages and typically involve test firing a liquid rocket to obtain results. This gives rise to the need to fabricate multiple chamber and nozzle assemblies. The report highlights the development of a closed loop control cooling system test rig to be used in testing the cooling of a liquid rocket engine. This will eliminate the need for static firing to test the cooling of rocket engine thus promoting rapid prototyping. The report highlights the design of the mechanical electrical and control components of the cooling system. The report features the full design as well as analysis and validation of the design.

Contents

Declaration	I
Table of contents	III
List of figures	VII
List of tables	IX
Nomenclature	X
Abstract	1
1 Introduction	1
1.1 Background	1
1.2 Problem statement	2
1.3 Objectives	2
1.3.1 Main objectives	2
1.3.2 Specific objectives	2
1.4 Justification of the study	3
1.5 Scope	3
1.6 Expected outcomes	3
2 Literature Review	4
2.1 Liquid rocket engine operation	4
2.1.1 Introduction	4
2.1.2 Nozzle design and isentropic flow	5
2.1.3 Rocket engine testing	7
2.2 Need for cooling	8

2.3	Types of cooling	9
2.3.1	Film cooling	9
2.3.2	Ablative cooling	10
2.3.3	Radiation cooling	10
2.3.4	Regenerative cooling	11
2.4	Heat transfer in the combustion chamber	11
2.5	Factors affecting the choice of cooling method	17
2.6	Dynamic cooling	18
2.7	Design considerations for cooling	18
2.7.1	Material selection	18
2.7.2	Selection of coolant	19
2.7.3	Selection of cooling passages geometry	20
2.7.4	Pressure drop in the cooling system	22
2.8	Water cooling on test stands	22
2.9	Gap analysis	23
3	Methodology	24
3.1	Outline	24
3.2	Mechanical module	24
3.2.1	Introduction	24
3.2.2	Combustion chamber subsystem	25
3.2.3	Cooling assembly subsystem	34
3.2.4	Coolant plumbing subsystem	41
3.3	Electrical Module	46
3.3.1	Design requirements	46
3.3.2	Pump selection	47
3.3.3	Conceptual design	47
3.3.4	Implementation of the design	48
3.3.5	Data collection	50

3.3.6	Data analysis	51
3.4	Control module	52
3.4.1	Design requirements	52
3.4.2	Control algorithm	53
3.4.3	Data collection	55
3.4.4	Data analysis	56
4	Results	57
4.1	Mechanical module	57
4.1.1	Cooling system design	57
4.1.2	Design validation	60
Fluid flow analysis	60	
Thermo-structural analysis	62	
Heat transfer analysis	63	
4.2	Electrical module	66
4.3	Control module	68
5	Conclusion	69
Bibliography		70
Appendices		i
A	Part drawings	ii
B	Budget and timeplan	viii
B.1	Provisional budget	viii
B.2	Timeplan	ix
C	Programming Code	x
C.1	CEA output parser-Python code	x
C.2	Nozzle sizing code-Matlab code	xiii

List of Figures

Figure 2.1.1 Liquid rocket engine test stand schematic	8
Figure 2.3.1 Film cooling	10
Figure 2.3.2 Regenerative cooling	11
Figure 2.4.1 Temperature gradient of regeneratively cooled combustion chamber	14
Figure 2.7.1 Regenerative cooling geometry	21
Figure 2.7.2 Film cooling geometry	21
Figure 3.1.1 Modular representation of entire system	25
Figure 3.2.1 Nasa CEA Software	28
Figure 3.2.2 Graph of Temperature/Isp against O/F ratio	29
Figure 3.2.3 Chamber and nozzle conceptual design	29
Figure 3.2.4 Chamber geometry designed	30
Figure 3.2.5 Chamber part drawing	31
Figure 3.2.6 chamber geometry final	33
Figure 3.2.7 Cooling pipe geometry	38
Figure 3.2.8 Outer wall part drawing	39
Figure 3.2.9 Cooling manifold design	40
Figure 3.2.10 Cooling subsystem model	41
Figure 3.2.11 Piping system conceptual design	42
Figure 3.2.12 20l Plastic tank	44
Figure 3.2.13 Plumbing for cooling	45
Figure 3.3.1 Power distribution	49
Figure 3.3.2 Pump circuitry	50

Figure 3.3.3 Heater circuit	51
Figure 3.3.4 Power control.	52
Figure 3.4.1 Program flow chart	55
Figure 4.1.1 Liquid engine geometry	58
Figure 4.1.2 3D Engine assembly	59
Figure 4.1.3 Completed mechanical assembly	59
Figure 4.1.4 Fluid flow analysis- Pressure	60
Figure 4.1.5 Fluid flow analysis- Velocity	61
Figure 4.1.6 Thermo-structural analysis- Stress analysis	62
Figure 4.1.7 Thermo-structural analysis- Volumetric analysis	63
Figure 4.1.8 Uncooled wall temperature	64
Figure 4.1.9 Wall temperature-cooled	65
Figure 4.2.1 Electronic design	67
Figure 4.3.1 Human interface	68
Figure A.0.1Back bracket	iii
Figure A.0.2Back bracket-2	iv
Figure A.0.3Bracket-1	v
Figure A.0.4outer shell	vi
Figure A.0.5Support	vii

List of Tables

Table 2.7.1 Properties of common rocket materials	19
Table 3.2.1 Common propellant combinations	27
Table 3.2.2 Comparison of copper and stainless steel	31
Table 3.2.3 Properties of Ethanol as a coolant	36
Table 3.2.4 Tube Material selection	37
Table 3.4.1 Experimental data outputs and outputs	56
Table 4.1.1 Boundary conditions fluid flow analysis	60
Table 4.1.2 Boundary conditions fluid flow analysis	62
Table 4.1.3 Cooling system Model Parameters	65
Table 4.2.1 Power budget	66
Table B.1.1Budget	viii
Table B.2.1Time plan	ix

Nomenclature

The next list describes several symbols that will be later used within the body of the document

- A/C Alternating Current
- CAD Computer Aided Design
- CEA Chemical Equilibrium and Applications
- CFD Computational Fluid Dynamics
- GOX Gaseous Oxygen
- LCD Liquid Crystal Display
- O/F Oxidizer to Fuel ratio
- PWM Pulse Width Modulation
- RPA Rocket Propulsion Analysis

Chapter 1

Introduction

1.1 Background

A rocket is any type of jet propulsion vehicle that carries propellants required for combustion and subsequent development of thrust. The propellants are usually either in solid or liquid state. Combustion occurs in a part of the rocket referred to as the rocket engine.

The rocket engine generates thrust through this aforementioned combustion. Here a release of thermal energy is derived from the chemical reactions of the propellants. High temperature and high pressure gases result from the combustion of the propellants. These gases are then ejected at the rocket nozzle at high velocity [1].

Liquid rocket engines are fed with liquid propellants stored under pressure from tanks and into a thrust chamber. The type of propellant used is either a bipropellant or monopropellant. A bipropellant consists of a liquid oxidizer and a liquid fuel. A monopropellant contains both oxidizing and fuel species [2].

The combustion temperatures in a liquid rocket engine are very high and can be over 3000 °C. This is also accompanied by a high heat transfer rate from the gases to the chamber wall.

1.2 Problem statement

An important part of rocket development is iterative testing to find the most optimal parameters for each rocket flight. Testing of the cooling system of a liquid rocket engine or various coolants to be used should not necessarily involve fabrication of a new thrust chamber.

Currently testing of the cooling system of a rocket engine requires performing of a static firing test. This leads to having a damaged thrust chamber should the cooling system not work on the first time of asking.

Damaging a thrust chamber as a result of failure due to high temperatures leads to the need to fabricate a new thrust chamber which is resource consuming. As such there is need for a part of the test stand that is dedicated to cooling which would allow for dynamic changing of the cooling rate. To solve this a cooling system test rig with closed loop control was designed to allow for testing without the need for static firing.

1.3 Objectives

1.3.1 Main objectives

To design and develop as part of a test rig, a closed loop control cooling system for a liquid rocket engine.

1.3.2 Specific objectives

1. To design and develop a mechanical structure for a thrust chamber with cooling facilities.
2. To design and develop an electrical system to power the sensors controller and actuator.

3. To develop and implement a control algorithm to achieve closed loop control of the cooling process.
4. To test the cooling system.

1.4 Justification of the study

Developing a closed loop control cooling system of a liquid rocket engine to be deployed on a test rig will eliminate the need to have static firing to test the efficiency of the onboard cooling system. This will reduce the strain on resources for iterative testing. The data points obtained from the testing will thereby be used to optimize the onboard cooling system.

1.5 Scope

This project will focus on developing a thrust chamber and a cooling system as part of a test rig specifically for the aforementioned thrust chamber.

1.6 Expected outcomes

The expected outcomes are:

1. Mechanical structure with consisting of a combustion chamber, nozzle and plumbing mechanism for cooling.
2. Electrical design to power the electrical system and transmit sensor values and control signals.
3. A control algorithm to stabilize performance of the cooling system.

Chapter 2

Literature Review

2.1 Liquid rocket engine operation

2.1.1 Introduction

Rocket propulsion systems can be classified according to their energy source type that is: chemical, nuclear, solar. Chemical propulsion systems are the most prevalent and they involve combustion to produce high energy exhaust gases. The exhaust gases are thermodynamically expanded to produce a high velocity exhaust whose reaction force is thrust. Chemical propulsion systems include solid propellant, liquid propellant and hybrid propellant systems. A propellant refers to the chemicals that undergo combustion in the propulsion system. If a system uses one single propellant it is referred to as a monopropellant system while if it uses two propellants it is referred to as a bipropellant system. Bipropellant systems comprise of an oxidizer and fuel. Liquid propellant systems offer the highest energy density. Liquid rocket engines are chemical propulsion systems where the propellants are either in liquid or gaseous form. The efficiency of a chemical propulsion system refers to its ability to convert the stored chemical energy of the propellants to kinetic energy of the exhaust gases.

2.1.2 Nozzle design and isentropic flow

A combustion chamber is designed to sustain combustion at the a specified pressure and propagate reacted gases towards the nozzle. The nozzle accelerates this flow to exhaust velocity and decreases the pressure of the flow to match the designed exit plane pressure. This operation is governed by the following assumptions [2]:

1. The working fluid is homogeneous in composition.
2. All the species of the working fluid are treated as gaseous. Any condensed phases (liquid or solid) add a negligible amount to the total mass.
3. The working fluid obeys the perfect gas law.
4. There is no heat transfer across any and all gas-enclosure walls; therefore, the flow is adiabatic.
5. There is no appreciable wall friction and all boundary layer effects may be neglected.
6. There are no shock waves or other discontinuities within the nozzle flow.

The above assumptions enable us to use isentropic flow relations in the nozzle. Stagnation conditions occur at the chamber where the pressure and the temperature at maximum level and the flow velocity is assumed to be zero. As the flow expands isentropically the pressure and temperature drop while the velocity increases. In a typical de Laval nozzle (one with a converging and diverging section) the flow before the throat (the narrowest part of the nozzle) is subsonic while flow after the throat is supersonic. Thus given the equation of rocket operation as equation 2.1.1 [2].

$$F = \dot{m}v_e + (p_e - p_o)A_e \quad (2.1.1)$$

where

F = Thrust

\dot{m} =mass flow rate

v_e = velocity of exhaust gases at exit

p_e = pressure of the exhaust gases at exit

p_o = ambient pressure

A_e =area of the exit plane Assuming that the pressure at the exit plane is equal to the ambient pressure then:

$$F = \dot{m}v_e \quad (2.1.2)$$

Since the flow is isentropic equation 2.1.3 [2] may be shown to hold between any two nozzle sections x and y.

$$\frac{T_x}{T_y} = \left(\frac{p_x}{p_y} \right)^{\frac{k-1}{k}} = \left(\frac{v_y}{v_x} \right)^{k-1} \quad (2.1.3)$$

where

T = temperature

p = pressure

v =velocity

$k = \frac{C_p}{C_v}$ and as function of the combustion reaction

C_p = Specific heat at constant pressure

C_v = Specific heat at constant volume

The above equation demonstrates the relation between pressure and velocity at any point in the nozzle. As this flow is isentropic the pressure at any point x is a factor of the ratio Area of point x and the throat Area. The thrust and the area can be related via the equation 2.1.4 [2].

$$C_F = \frac{F}{p_1 A_t} \quad (2.1.4)$$

where

$$C_F = \text{thrust co-efficient}$$

$$F = \text{Thrust}$$

$$p_1 = \text{chamber pressure}$$

$$A_t = \text{throat area}$$

The thrust co-efficient is a factor of the propellants chosen and can be found using such software as Nasa CEA. With the throat area determined the geometry can be determined using isentropic flow equation 2.1.5 [2].

$$\frac{A}{A_t} = \left(\frac{k+1}{2} \right)^{-\frac{k+1}{2(k-1)}} \left[\frac{1 + (\frac{k-1}{2})M^2}{M} \right]^{\frac{k+1}{2(k-1)}} \quad (2.1.5)$$

where

M = local Mach number of the gases.

2.1.3 Rocket engine testing

To determine the rocket engine performance before the actual flight several tests are carried out on a test stand as represented in Figure 2.1.1 [4]. Figure 2.1.1 demonstrates a bipropellant liquid rocket engine. Gaseous nitrogen in the green tank is used to pressurize the fuel towards the combustion chamber. The fuel used is ethanol (C_2H_5OH) which is stored in the fuel tank. Gaseous oxygen is the other propellant and is also used in the ignition unit. The ignition unit uses a small amount of the propellant mixture which is ignited when it reaches the igniter at the entrance of the combustion chamber. Water is pumped around the combustion chamber for cooling purposes. The entire schematic consists of manual, relief and solenoid valves that are used to control fluid flow. Flow meters are used to measure the rate of fluid flow throughout the system [3]. The performance of the rocket engine is tested via a static test. The engine is clamped in place and

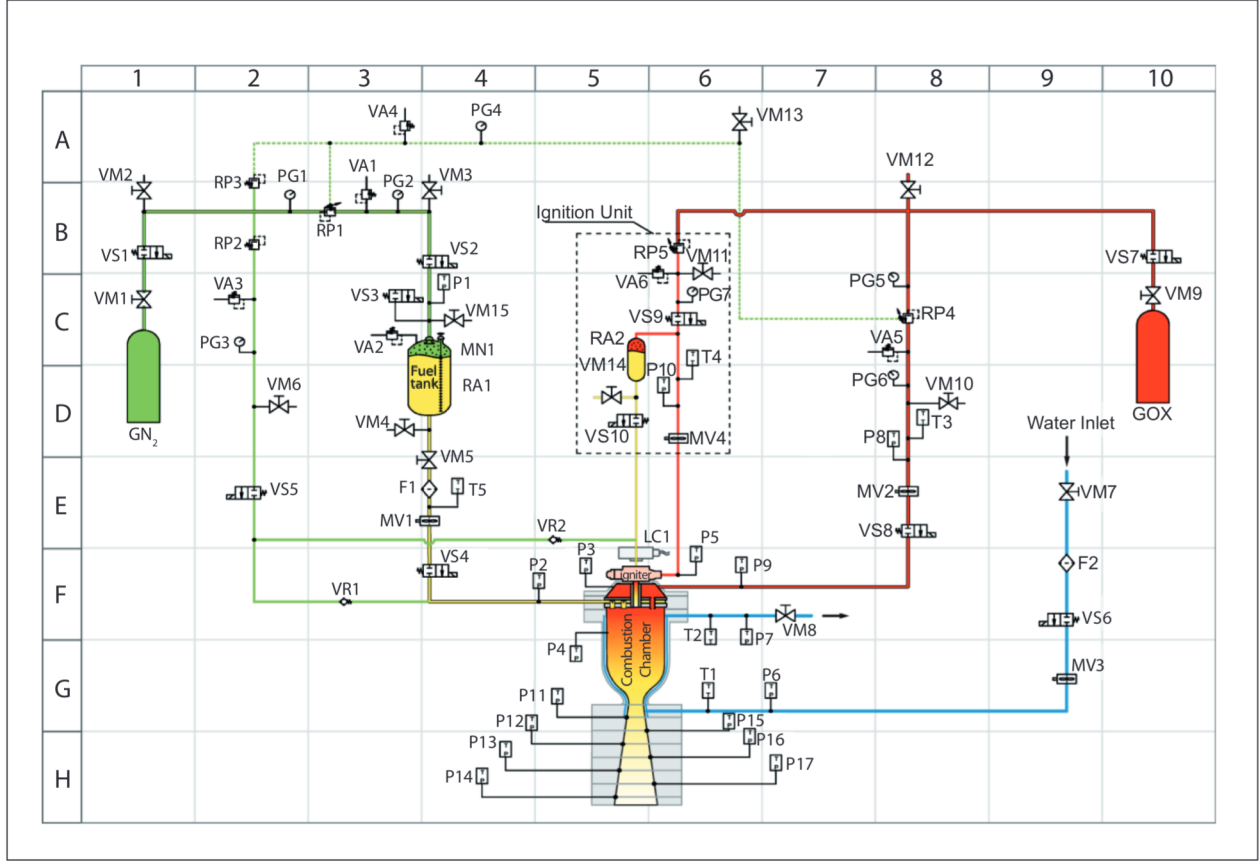


Figure 2.1.1: Liquid rocket engine test stand schematic[3]

ignited. The thrust produced is measured by force measuring devices such as load cells. The propellant feed system provides the propellant for the static firing [5].

2.2 Need for cooling

During rocket operation the propellants, oxidizer and the fuel, undergo combustion in the combustion chamber of the rocket. The reaction results in hot gases and is meant to liberate the chemical energy of the propellants, converting it into heat and pressure. If done stoichiometrically, combustion temperatures can range between 2500 to 3600 K for common propellants [2]. The combustion chamber and nozzle are designed to convert the

heat and pressure generated into kinetic energy. The exhaust gases leave the nozzle at high velocity which generates a reaction force, thrust, which propels the rocket forward.

Not all the heat produced by the combustion is converted to kinetic energy. Some heat is absorbed by the combustion chamber and during nozzle operation a lot of the heat is dissipated to the nozzle. This is disadvantageous since most of the materials used to make rocket combustion chambers and nozzles lose strength as the temperature increases [6]. The chamber and nozzle also experience high pressure and if temperatures are allowed to rise this could lead to the material of the combustion chamber or nozzle failing or melting [7].

2.3 Types of cooling

Uncooled chamber walls can be used for a short duration up to a few seconds. For longer duration applications a cooling method has to be employed. Cooling methods can be characterized into two; steady state cooling methods and transient methods [2]. In steady state cooling methods heat transfer rates and chamber temperatures reach thermal equilibrium. This include regenerative cooling and radiation cooling. In transient methods heat transfer rates and chamber temperatures do not reach thermal equilibrium, these methods include ablative cooling and film cooling [8].

2.3.1 Film cooling

Film cooling controls the chamber wall temperature by interposing a layer of coolant fluid between the surface to be protected and the hot gas stream from combustion as shown in Figure 2.3.1 [9]. This results in lower wall temperatures. It is used in high heat fluxes and in combination with steady state cooling methods such as regenerative cooling [10].

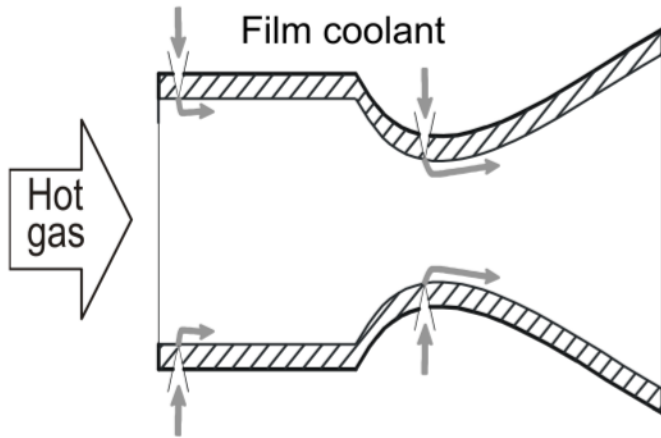


Figure 2.3.1: Film cooling [11]

2.3.2 Ablative cooling

Here select materials are used for sacrificial cooling by progressive endothermic disintegration of fiber-reinforced organic material and mass flow of pyrolysis gases away from the heated surface. This blocks heat transfer to the outer surface of the abrasive material [12]. This method suffers from two major challenges that is; the chamber is not reusable as the wall material decomposes or disintegrates, the chamber geometry changes during operation thus optimum performance is not maintained.

2.3.3 Radiation cooling

The chamber is made of high temperature material. Heat is transferred away from the surface of the outer thrust chamber wall [1]. When it reaches thermal equilibrium, this wall may glow red or white as it radiates heat away to the surrounding medium or to empty space. This method is often used for small engines characterized by low pressure and low thermal fluxes [2].

2.3.4 Regenerative cooling

The fuel enters the cooling paths at the nozzle exit of the thrust chamber passes through the throat area and exits at the injector face as shown in Figure 2.3.2 [13]. This method is often used in applications with high chamber pressures and high heat transfer rates [14].

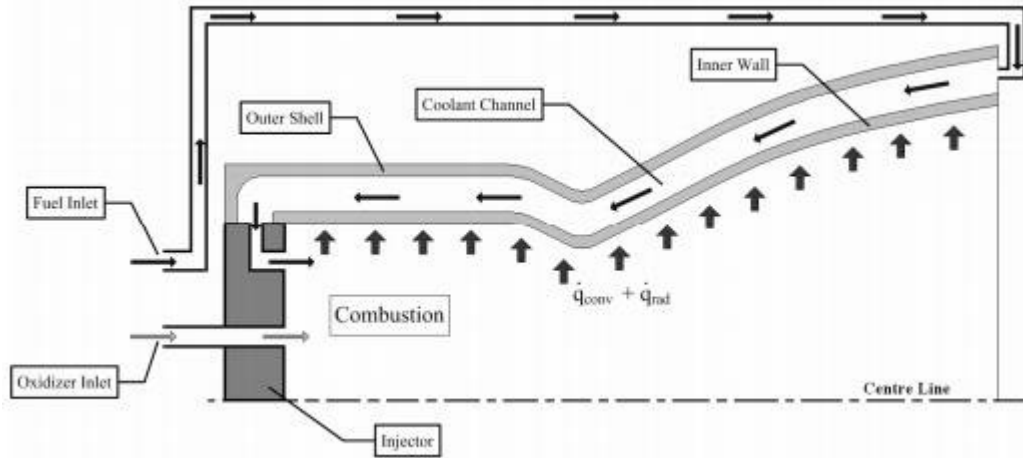


Figure 2.3.2: Regenerative cooling[15]

2.4 Heat transfer in the combustion chamber

Heat transfer analysis in the combustion chamber provide a useful guide in design, testing, and failure investigations [2]. Heat transfer analysis is different for steady state and transient cooling methods. Heat transfer analysis can be done by Finite Element Analysis (FEA) software. Heat transfer in the combustion chamber involves convection from the gases and propellants in the chamber, conduction by the chamber and nozzle and radiation from the surface of the nozzle and the chamber to the atmosphere. A majority of the heat transferred from the hot gases produced during combustion is transferred to the wall of the combustion chamber is done by convection. Conduction makes up a very small percentage with radiation accounting for between 5 - 35% [16] [17]. The basic relation of

the heat transfer from the combustion gases to the wall of the combustion chamber can be expressed in equation 2.4.1 [16].

$$q = h_g(T_{aw} - T_{wg}) \quad (2.4.1)$$

where:

q = Heat flux; heat transferred across the stagnant gas film per unit surface per unit time.

h_g = Gas side heat transfer co-efficient.

T_{aw} = Adiabatic temperature of the gas.

T_{wg} = Hot-gas-side local chamber-wall temperature

The gas film co-effecient is given by equation 2.4.2 [16].

$$h_g = \left[\frac{0.026}{D_t^{0.2}} \left(\frac{\mu^{0.2} C_p}{Pr^{0.6}} \right)_{ns} \left(\frac{(P_c)_{ns} g}{c^*} \right) \left(\frac{D_t}{R} \right)^{0.1} \right] \times \left(\frac{A_t}{A} \right)^{0.9} \times \sigma \quad (2.4.2)$$

where

D_t = Diameter of nozzle throat

μ = Viscosity

C_p = Specific heat at constant pressure

Pr = Prandtl number

$(P_c)_{ns}$ = Stagnation pressure

c^* = characteristic velocity

R = Nozzle radius of curvature at throat

A = Area along chamber axis

σ = Correction factor for property variations across the boundary layer

A_t = Area of nozzle throat

The adiabatic temperature of the combustion gas at any given location in the thrust chamber can be obtained from equation 2.4.3 [16].

$$T_{aw} = (T_c)_{ns} \left[\frac{1 + r(\frac{\gamma-1}{2})M_x^2}{1 + (\frac{\gamma-1}{2})M_x^2} \right] \quad (2.4.3)$$

where:

$(T_c)_{ns}$ = Nozzle stagnation temperature

M_x = local Mach number

r = Local recovery factor

R = Effective recovery factor (from 0.90 to 0.98)

The local recovery factor represents the ratio of the frictional temperature increase to increase caused by adiabatic compression. This may be determined experimentally or estimated from equations 2.4.4 and 2.4.5 [16].

$$r = 0.5P_r(\text{laminar flow}) \quad (2.4.4)$$

$$r = 0.33P_r(\text{Turbulent flow}) \quad (2.4.5)$$

Determination of gas side heat transfer co-efficient is a complex problem with data from analytical methods and experimental methods disagreeing [2] [17]. The disagreement is largely due to the initial assumptions of analytical methods than do not account for turbulent combustion pressure and the changing localised gas composition and temperature. The determination of heat flow is important in the analysis of the method of cooling to be chosen and the specific parameters.

In the case of regenerative cooling as shown in Figure 2.4.1 the general heat transfer to the walls can be treated as a problem of steady state heat transfer in series. It

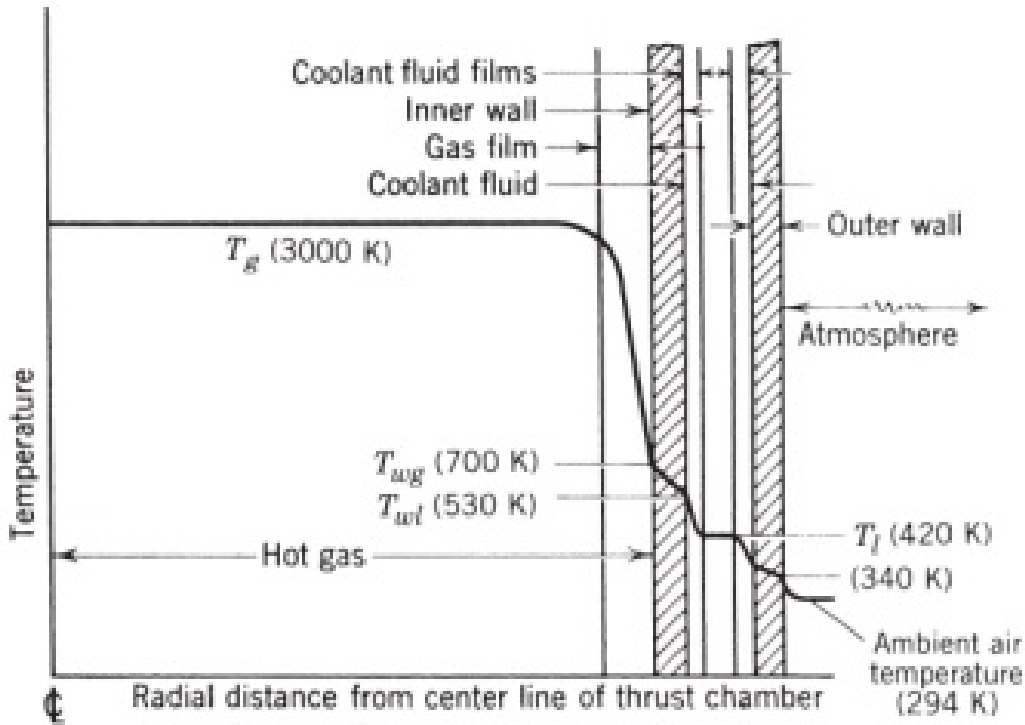


Figure 2.4.1: Temperature gradient of regeneratively cooled combustion chamber [2]

is a combination of convection at the boundaries of the flowing fluids and conduction through the chamber walls. The heat transfer involves convection through the gas film produced during combustion. The gas side heat co-efficient is found as detailed above [18]. This is followed by conduction through the wall of the chamber associated with the wall conduction co-efficient expressed by equation 2.4.6 [2].

$$\frac{Q}{A} = -k \frac{dT}{dL} = -k \frac{\Delta T}{t_w} \quad (2.4.6)$$

where:

Q = heat transferred to a surface area A

$\frac{dT}{dL}$ = temperature gradient

t_w = wall thickness and

k = thermal conductivity

The negative sign indicates that the temperature decreases as the thickness increases. This co-efficient is governed by the thickness of the wall and the thermal conductivity of the wall material. The third co-efficient in the series is the liquid film co-efficient of the coolant. Heat is transferred from the wall to the flowing coolant. The liquid film co-efficient denoted as h_l and is found as shown in equation 2.4.7 [16]:

$$h_l = \frac{kNu}{d} \quad (2.4.7)$$

where: Nu is Nusselts number and is given by equation 2.4.8 [16]:

$$Nu = C_1 Re^{0.8} Pr^{0.4} \left(\frac{\mu}{\mu_w} \right)^{0.14} \quad (2.4.8)$$

where:

C_1 = Constant (different values for various coolants)

Nu = Nusselt number

Re = Reynolds number = $\frac{\rho V_{co} d}{\mu}$

Pr = Prandtl number = $\frac{\mu C_p}{k}$

μ = Coolant viscosity at bulk temp.

μ_w = Coolant viscosity at coolant sidewall temperature.

d = Coolant passage hydraulic diameter.

k = Coolant thermal conductivity.

ρ = Coolant density.

V_{co} = Coolant velocity.

C_p = Coolant specific heat at constant pressure, These equation of convection heat transfer in turbulent flows are largely empirical, and can vary largely with actual experimental values. Th above equation is base on Bartz co relation which is semi-empirical. It

offers a better estimation but actual values may vary. The general heat flux(q) can thus be calculated as in equation 2.4.9 and 2.4.10 [16]:

$$q = H(T_g - T_l) = \frac{Q}{A} \quad (2.4.9)$$

where:

q = heat transferred per unit area per unit time

T_l =the absolute coolant liquid temperature

and

$$H = \frac{1}{\frac{1}{h_g} + \frac{t}{k_w} + \frac{1}{h_l}} \quad (2.4.10)$$

where:

k_w = thermal conductivity of chamber wall

t = wall thickness

From the above equations it is possible to calculate the wall temperature. This relationship and the above bring a number of factors for cooling into the foreground[19]:

- The specific temperature of the coolant
- The specific heat capacity of the coolant
- The thickness of the chamber wall
- The nature of the propellants
- The nature of combustion including temperature and pressure
- The properties of the material used to make the chamber wall

2.5 Factors affecting the choice of cooling method

The selection of the best cooling technique to use is specific to the design of the chamber, however there are some general rules that aid in this selection [16] [20] [21]:

1. Propellants

The properties of the propellants after combustion such as temperature, specific heat, specific weight, viscosity have an effect on the heat-transfer rate and thus the choice of cooling to be used. The heat conductivity of the propellants as well as their flow rate is also determines whether they can be used for regenerative,film or transpiration cooling [22].

2. Chamber Pressure

Higher pressures are associated with higher combustion- exhaust gases flow rate per unit area of the combustion chamber. This leads to increased heat transfer to the chamber. Thus for high chamber pressures a combination of cooling methods is often employed.

3. Propellant feed system

The type of propellant feed system used determines how much pressure is available for cooling. For turbo pump fed systems there is a high pressure budget meaning that it is convenient to use regenerative cooling. For pressure fed systems which have a lower pressure budget which may not accommodate regenerative cooling other cooling methods such as ablative,film and radiation are preferred.

4. Thrust chamber configuration

The shape of the combustion chamber determines the flow rate of the exhaust gases after combustion. Higher flow rates increase the rate of heat transfer. Spherical chambers offer the best cooling efficiency but are difficult to machine.

5. Thrust chamber construction material

The choice of material for the combustion chamber will greatly affect the chosen cooling system. If the engine is small and the material chosen is of high conductivity then heat sinking can be used. Strength at elevated temperatures and the heat conductivity of the material affect the choice of cooling. For film cooling the material should have a high working temperature range. The success of ablative cooling wholly depends on the type of material chosen.

2.6 Dynamic cooling

Cooling can be done at a constant or varying rate. Dynamic/variable cooling can be achieved by varying the mass flow rate of the coolant. This is highlighted by equation 2.4.6 where the liquid film co-efficient (h_l) depends on the Reynolds number which is affected by the mass flow rate of the coolant. An increase in the mass flow rate with a subsequent increase in velocity leads to an increase in the overall heat transfer coefficient [23].

2.7 Design considerations for cooling

2.7.1 Material selection

The material to be used to develop the combustion chamber and nozzle as well as the cooling jacket has a considerable effect on the cooling[6]. The material for design of the combustion chamber should have the following characteristics:

- High thermal conductivity
- High melting point

- High specific thermal strength at high temperatures
- High wear resistance against erosion by exhaust gases
- Machinability

The properties of some common materials used in rocketry are as shown in Table 2.7.1 [24].

Table 2.7.1: Properties of common rocket materials [24]

Metal	Density (g/cm^3)	Melting point	Cu 100 therm. conduc- tivity	chamber hard- ness	tensile strength at 1000 °C	nature of oxide at high temp
Aluminium	2.7	658	55	2.9	liquid	refractory
Duralumin	2.8	550	30	3.5	liquid	refractory
Copper	8.9	1083	100	3.5	10 MPa	powdery
Iron	7.9	1538	30	4.5	18 MPa	powdery
Stainless steel	7.8	1250	5	5.5	42 MPa	partial refrac- tory

2.7.2 Selection of coolant

Depending on the type of cooling employed the type of coolant changes. For ablative cooling the material may be a solid ceramic. For film cooling the fuel is the coolant. For transpiration cooling For regenerative cooling the coolant may be either the oxidizer or the fuel. Depending on the mass flow rate and the specific heat carrying capacity, one of the propellants is chosen. Despite the large temperature difference offered by liquid oxygen it offers compatibility issues [6].

2.7.3 Selection of cooling passages geometry

The geometry of the cooling passages has a large effect on the velocity of the coolant and the mass flow rate of the coolant. Thus the geometry of the cooling passages affect the heat transfer co-efficient to the coolant.

- **Regenerative cooling**

The cooling passages in regenerative cooling allow the flow of coolant through them during combustion. The coolant absorbs heat from the combustion chamber and this is used to preheat the propellant. The various types of cooling passages are as shown in figure(fig number). Figure 2.7.1(a) shows circular tubes bounded by an outer shell. The circular tubes make up the combustion chamber and are reinforced by the outer shell. Figure 2.7.1(b) shows elongated tubes similar in operation to circular tubes with the only difference being the geometry of the passage. They are more effective than circular tubes due to the high aspect ratio. Figure 2.7.1(c) shows milled cooling channels as cooling passages. The assembly comprises of an inner combustion chamber than has milled channels on the outer side. The channels are covered by an outer shell which forms the closed geometry for cooling.

The second technique involves the milling of rectangular cooling channels along the contour of a thick thrust chamber as shown in Figure 2.7.1.

- **Film cooling**

This type of cooling can be achieved using two techniques[25] The first involves the use of the injector. The injector configuration can be used to spray propellant onto the walls of the combustion chamber. The second method involve drilling holes or slots onto the wall of the combustion chamber to introduce the coolant. This is as shown in Figure 2.7.2.

- **Dump cooling**

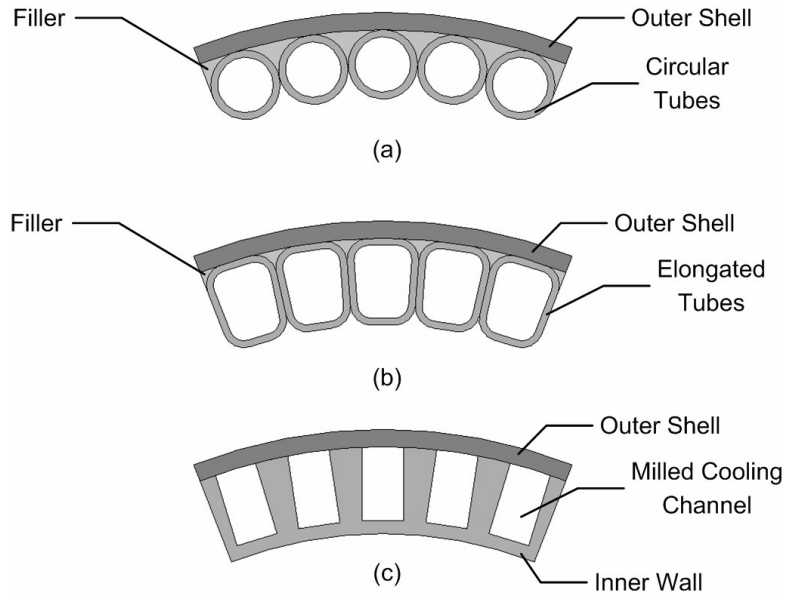


Figure 2.7.1: Regenerative cooling geometry[2]

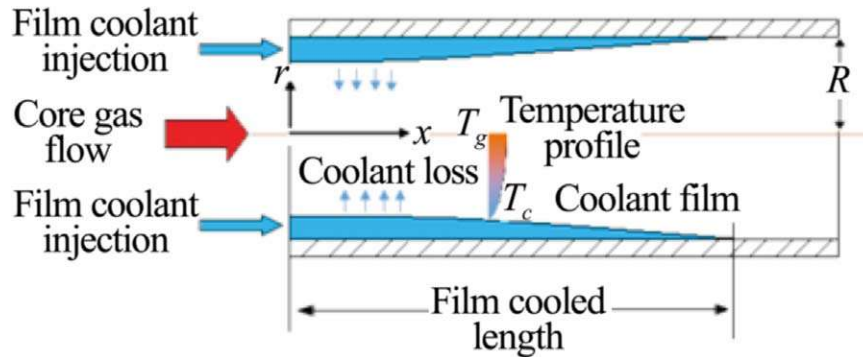


Figure 2.7.2: Film cooling geometry[25]

Dump cooling involves the uses of cooling passages similar to those of regenerative cooling. The direction of coolant flow in dump cooling is opposite to that of regenerative cooling. The coolant is not used in combustion as in regenerative cooling.

2.7.4 Pressure drop in the cooling system

The pressure drop in the cooling system is a major factor in design. It affects the choice of supporting machinery for the liquid engine such as turbo pumps. The pressure in the cooling channels also affects the rate of heat transfer in the cooling channels. The pressure drop in the cooling system can be calculated as shown in equation 2.7.1 [16].

$$\frac{\Delta p}{\rho} = \frac{1}{2} f v^2 \left(\frac{L}{D} \right) \quad (2.7.1)$$

where:

Δp = the friction pressure loss.

ρ = the coolant mass density.

L = the length of coolant passage.

D = the equivalent diameter.

v = the average velocity in the cooling passage.

f = a friction loss coefficient.

2.8 Water cooling on test stands

Here the temperature of the chamber wall is kept at a controlled temperature by running water at a constant rate through the cooling jacket. This is the same cooling jacket that would be used with a coolant during the flight of the rocket [3]. This process uses a constant mass flow rate which is determined using equation 2.8.1 [26].

$$m_w = \frac{1.1\pi q_{cw}(D_c + 2t_{cw})L_c}{c_w \Delta T_w} \quad (2.8.1)$$

where:

q_{cw} = Average heat transfer rate of chamber material.

D_c = Combustion chamber diameter.

t_{cw} = Thrust Chamber wall thickness.

L_c = Combustion chamber length.

c_w = Coolant water specific heat capacity.

ΔT_w = Desired water temperature value.

2.9 Gap analysis

The development of an appropriate cooling system for a liquid rocket engine is affected by a number of factors such as manufacturing constraints and engine specifications. For an efficient cooling system to be developed there is a necessity to test the developed cooling system. Existing systems require static tests. Static tests are resource intensive as they require firing the engine to test engine performance as well as cooling efficiency performance. Failure of the cooling system can be detrimental to the engine. There is need to develop a test rig that will be able to test cooling system performance without the need for static firing. This will present a cheap and efficient way of testing the cooling system.

Chapter 3

Methodology

3.1 Outline

This section highlights the design of the liquid rocket engine, the cooling system and the test stand set up. The section highlights the mechanical, electrical and software design considerations and implementation. The system can be represented in modules as shown in Figure 3.1.1.

3.2 Mechanical module

3.2.1 Introduction

The design of the mechanical module of the cooling system test rig was divided according to the following subsections:

1. The combustion chamber subsystem
2. Cooling assembly subsystem
3. Fluid delivery subsystem

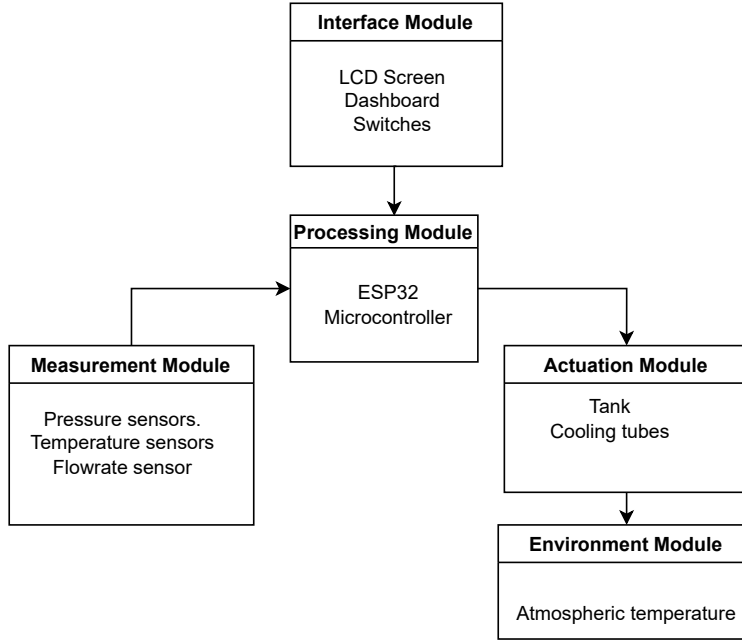


Figure 3.1.1: Modular representation of entire system

3.2.2 Combustion chamber subsystem

This subsystem is required to facilitate the combustion of the propellants(oxidizer and fuel). The products of the combustion are usually at high pressure and temperature and the combustion chamber subsystem is required to convert the high thermal energy and pressure into kinetic energy of the exhaust gases. This kinetic energy results into the thrust of the rocket. This subsystem comprises of the combustion chamber and the nozzle. The geometry of the combustion chamber and the nozzle have a great effect on the rocket performance and hence great care should be taken on the design. The design followed the following steps:

1. Design requirements

The design requirements of the combustion chamber subsystem can be listed as:

(a) Functional Requirements

- i. The design should be able to handle the high temperatures of combustion which can be as high as 3300K as well as high pressure of combustion.
- ii. The design should offer high efficiency in the conversion of thermal energy and pressure into kinetic energy.
- iii. The design should produce steady in-compressible flow without flow separation and supersonic flow at the exit.

(b) Non-functional Requirements

- i. The design should be able to be fabricated using locally available fabrication methods.
- ii. The design should be easily integrated into the injector and test stand design of the Nakuja project.

2. Design considerations

The following were design considerations for the design:

- Required thrust
- Combustion pressure
- Combustion temperature
- Propellants used
- Fabrication considerations

3. Conceptual Design

The following steps were undertaken to generate a conceptual design:

- Selection of propellants

Table 3.2.1: Common propellant combinations [27]

Oxidizer	Propellant	Isp(s)
Liquid oxygen	Kerosene	250 to 270
Liquid oxygen	Ethanol	250 to 270
Hydrazine	Chlorine trifluoride	250 to 270
Liquid oxygen	fluorine-JP-4	270 to 330
Liquid oxygen	ozone-JP-4	270 to 330
Liquid oxygen	Hydrazine	270 to 330
Liquid oxygen	fluorine-JP-4	270 to 330
Fluorine	Hydrogen	300 to 385
Fluorine	Ammonia	300 to 385
Ozone	Hydrogen	300 to 385
Fluorine	Diborane	300 to 385

A number of propellants are available for rocket propulsion which have been adequately studied and performance mapped as shown in Table 3.2.1. The main consideration for the selection of propellants was availability locally and relative safety in handling. Cryogenic propellants are not available locally hence the oxidizer chosen was gaseous oxygen instead of liquid oxygen. Due to their availability and safety in handling, two fuels were considered, Kerosene and ethanol. Ethanol was chosen as it could be obtained with near 100% purity while the exact composition of Kerosene could not be determined.

- **Selection of specific Engine performance parameters**

As this project is part of the Nakuja project the following parameters were established as requirements.

- Chamber pressure = 2.0 Mpa
- Desired thrust = 2 kN

- **Selection of Oxidizer-Fuel ratio**

The oxidizer to fuel (O/F) ratio is an important parameter in the calculations to design the chamber geometry. The O/F ratio is also important in determining the mass flow rate of the propellants which also determines the cooling capability of the rocket. The determination of the O/F ratio requires determination of combustion parameters of the fuel and oxidizer. This was done using the NASA CEA software shown in Figure 3.2.2.

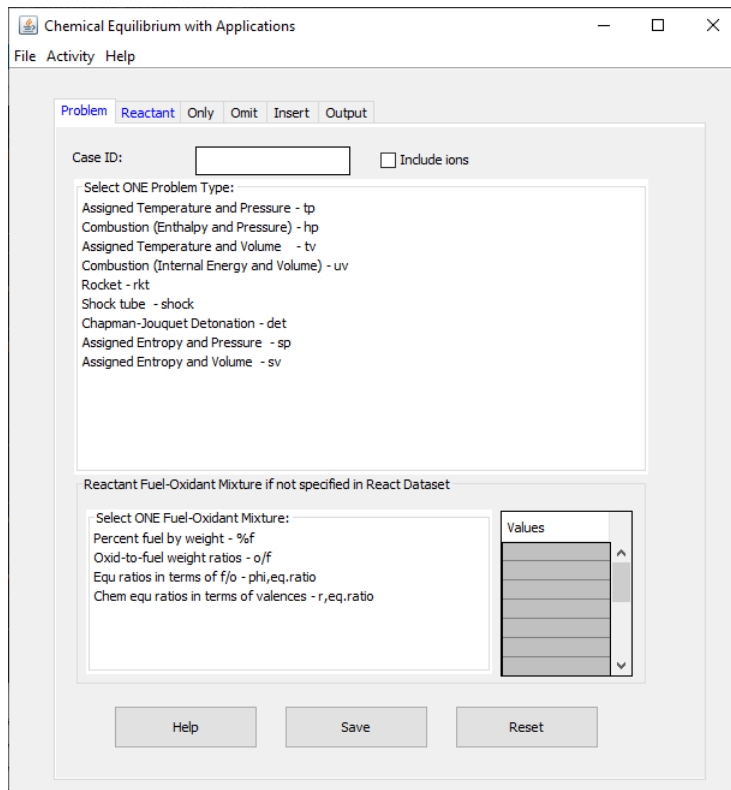


Figure 3.2.1: Nasa CEA Software

The software was able to generate data on various O/F ratios. A Python script was written to parse and data and generate graphs which would be used to pick the optimum O/F ratio. The main considerations for this selection were the specific Impulse (Isp) and the combustion temperature. The specific impulse is a measure of rocket performance and the higher the better. The combustion

temperature was required to be kept at a minimum to limit material stresses. The graphs generated are as shown in Figure 3.2.3.

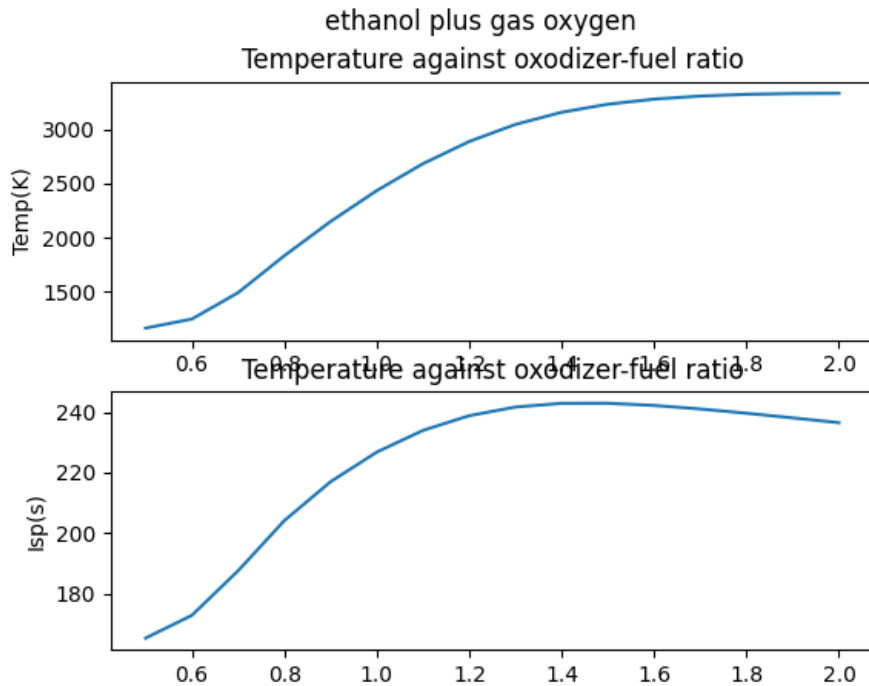


Figure 3.2.2: Graph of Temperature/Isp against O/F ratio

The optimum oxidizer to fuel ratio was chosen as 1.5. The conceptual design comprises a combustion chamber with a de Laval nozzle. This is as shown in Figure 3.2.3 which shows a simple converging, diverging section.

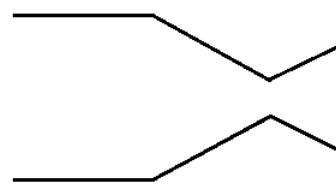


Figure 3.2.3: Chamber and nozzle conceptual design

4. Geometry Design

The isentropic flow equations were used to determine the geometry. We generated a script to handle the calculations as shown in Appendix C. The calculations were confirmed using Rocket Propulsion Analysis (RPA) software which was also used to generate the parabolic approximation nozzle dimensions. The generated geometry is as shown in Figure 3.2.4.

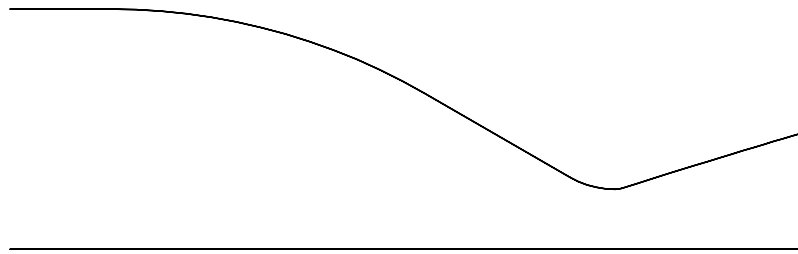


Figure 3.2.4: Chamber geometry designed

The geometry was produced in Autodesk Inventor and used to generate the combustion chamber. The generated drawing is as shown in Figure 3.2.5.

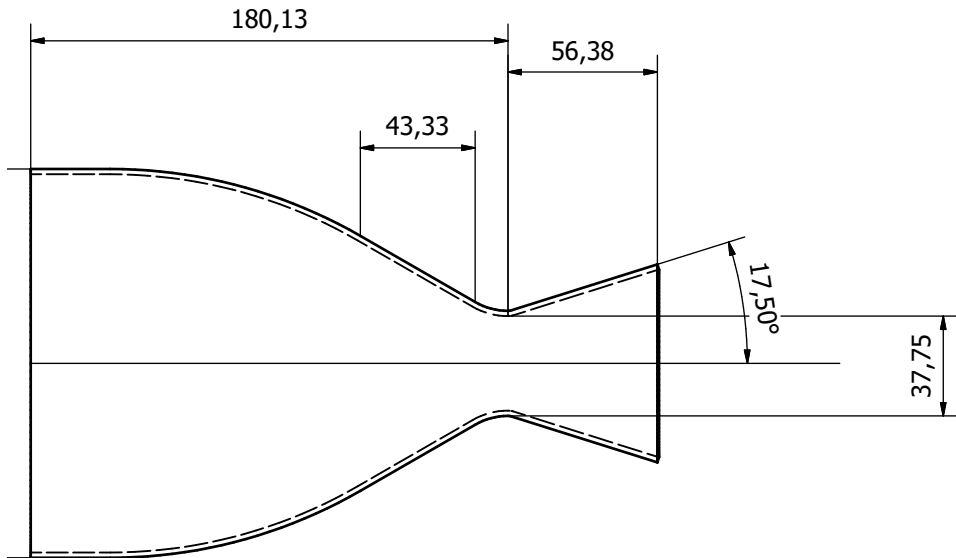


Figure 3.2.5: Chamber part drawing

5. Material selection

The following were requirements for the material to be selected for the chamber and nozzle:

- (a) High strength
- (b) High thermal conductivity
- (c) Machinability

The materials considered are as shown in Table 3.2.2:

Table 3.2.2: Comparison of copper and stainless steel

Material	Tensile strength(MPa)	Melting point(°C)	Thermal Conductivity
Oxygen Free Copper	221	1083	391 W/m-K
NARloy-Z	124	800	320 W/m-K
Stainless steel Grade 304	540	1400	16.2W/m-K

Stainless steel was chosen because of its high melting point which will offer less of a cooling requirement on the cooling system. Stainless steel is also much cheaper than Copper. The material chosen influenced the chamber geometry by determining the thickness of the chamber wall. The chamber wall is required to be thin to allow for effective heat transfer but still be strong enough to withstand the high combustion pressure. The design should also take into account the effect of elevated heat on the material. The chamber thickness was calculated as follows:

$$P_D = \frac{2 \times t \times fty \times 1000}{d \times s} \quad (3.2.1)$$

where:

t = thickness

fty = yield strength

d = chamber diameter

s = design safety factor

$$\begin{aligned} 2000 &= \frac{2 \times t \times 215 \times 1000}{143.01 \times 2} \\ t &= \frac{2000}{1503.39} \\ t &= 1.33 \end{aligned} \quad (3.2.2)$$

$$t \approx 2mm$$

The chamber was chosen to be 2 mm thick as shown in equation 3.2.2.

The final design of the chamber is as shown in Figure 3.2.6.

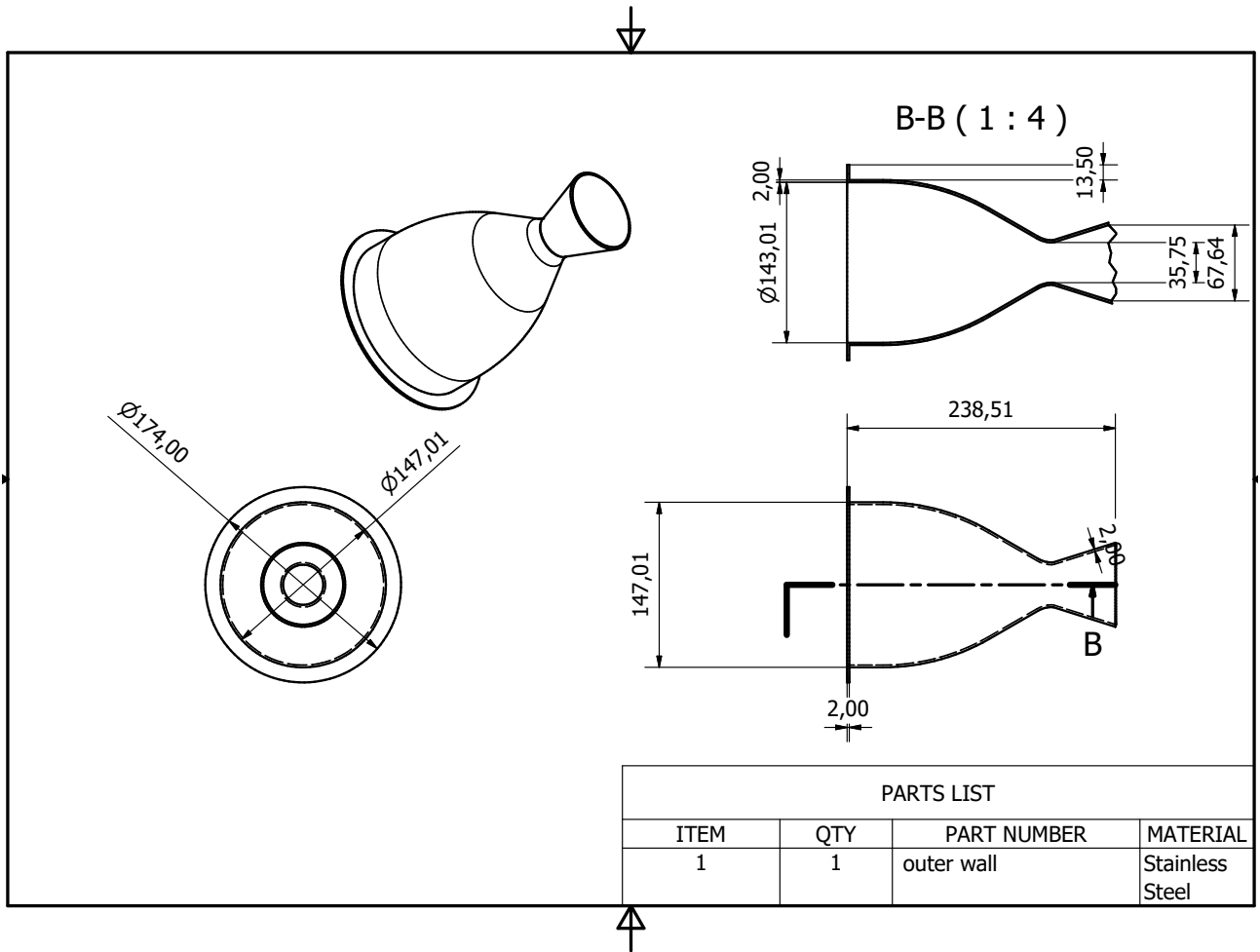


Figure 3.2.6: chamber geometry final

6. Data collection

Validation of chamber design was done to ensure that the design met the technical requirements and that it was safe. The following validation procedures were conducted on the design:

- Fluid flow analysis Flow through a rocket engine nozzle is considered isentropic that is; it is adiabatic and reversible. Isentropic flow calculations can be conducted to determine the pressure and velocity of exhaust gases at any point along the chamber geometry. This calculations are enhanced using CFD soft-

ware such as ANSYS. The developed geometry was analyzed to determine exit pressure and the presence of shock waves and flow separation. The procedure was as follows:

- (a) A 2D axis symmetrical model of the chamber wall was imported into ANSYS.
- (b) The geometry was subjected to meshing.
- (c) Boundary conditions were applied
- (d) The simulation was run with 4500 iterations

The results are presented in chapter 4.

- Thermo-structural analysis The inner wall of the rocket engine will be subjected to both high temperature and pressure. Thermo-structural analysis is a combination of thermal analysis as well as static structural analysis. This is used to determine stresses under both pressure and thermal loading. The procedure was as follows:

- (a) A 3D model of the inner wall was imported into ANSYS.
- (b) The material was set for model and meshing was conducted.
- (c) Data from fluid flow analysis was imported to apply pressure and thermal loading.
- (d) The simulation was run with 6000 iterations

The results are as presented in chapter 4.

3.2.3 Cooling assembly subsystem

The cooling assembly subsystem is required to take away heat from the engine during operation to prevent failure of the chamber wall. From the literature review, regenerative cooling was chosen for the engine. It presents the following advantages:

- It is a relatively efficient method of cooling.

- It enables a method of dynamic control thus can be optimized for flight.
- The fuel used is preheated thus increasing the energy of combustion.
- It is relatively easy to implement.

The cooling assembly subsystem comprises of the inlet manifold, the outlet manifold and the outer wall. The following describes the steps for designing the regenerative cooling assembly:

(a) **Design requirements**

The following were identified as design requirements for the cooling assembly subsystem:

- Functional requirements
 - i. The system should be able to provide adequate cooling to the engine to prevent failure.
 - ii. The system should be able to vary the rate of cooling to optimise fluid flow
 - iii. The system should limit the pressure drop across the cooling channels.
- Non-functional requirements
 - i. The system should be easy to implement.
 - ii. The system should not be bulky.

(b) **Design Considerations**

The following were design considerations for the cooling assembly subsystem:

- The combustion temperature of the propellants
- The enthalpy of the propellants
- The thermal conductivity, melting point and material of the combustion chamber,
- The pressure drop across the cooling channel.
- The type of regenerative cooling method implemented.

- The coolant and its properties.

(c) Conceptual Design

Following the requirements and design considerations of the subsystem, a regenerative cooling system using cooling tubes was proposed. Regenerative cooling was chosen due to its high efficiency. Cooling tubes were chosen because of fabrication constraints. The cooling tubes can be fabricated with the currently available resources.

(d) Selection of coolant

From the decision to use Gaseous Oxygen(GOX) and ethanol as the propellants, ethanol was chosen as the propellant to be used for regenerative cooling. Ethanol was used as it has a higher specific heat capacity than GOX. The pressure loss associated with GOX are much higher than that of ethanol. Some of the properties of ethanol are as listed in Table 3.2.3.

Table 3.2.3: Properties of Ethanol as a coolant [28]

Property	Value
Boiling point	78.37 °C
Melting point	-114.1 °C
Specific heat capacity	2.46 J/g°C
Thermal conductivity	0.17 W/m-K

(e) Cooling channels design

Cooling tubes were chosen as the channels for coolant to flow along the wall of the chamber to take away heat during combustion. The geometry of the cooling tubes was to be determined by available industrial standards. The design process began by identifying available cooling tubes. The following were identified as possible cooling tubes:

Copper tubes were chosen because of their ductility, thermal conductivity and relative availability. For this application the surface area of cooling needed to

Table 3.2.4: Tube Material selection [18]

Material	Thermal conductivity	Availability
Wrought Copper	320 W/m-K	Yes
Brass	147 W/m-K	No
Iron	80 W/m-K	Yes
Steel	16 W/m-K	Yes

be maximized to ensure effective cooling. To achieve this the smallest available size of tube was chosen to place as many as possible along the wall as closely as possible. The smallest available size of copper is 3/4 inch. This tube has an outer diameter of 0.375 inches. It has a inner diameter of 0.305 inches. The number of cooling tubes to be used was determined using equation 3.2.3.

$$N = \frac{2 \times \pi(R + r)}{d + c}$$

$$N = \frac{2 \times \pi(17.875 + 4.7625)}{9.525 + 5} \quad (3.2.3)$$

$$N = 9.79$$

$$N \approx 10$$

where

N = Number of cooling tubes

R = Throat Radius

r = Radius of cooling tube

d = diameter of cooling tube

c = clearance for welding

The selected copper tubes are to be bent to match the geometry of the chamber.

This is as shown:

(f) Inlet and Outlet manifold design

The purpose of this manifold is to deliver coolant to the cooling tubes as well as to take fluid away from the cooling tubes. Coolant is delivered through a

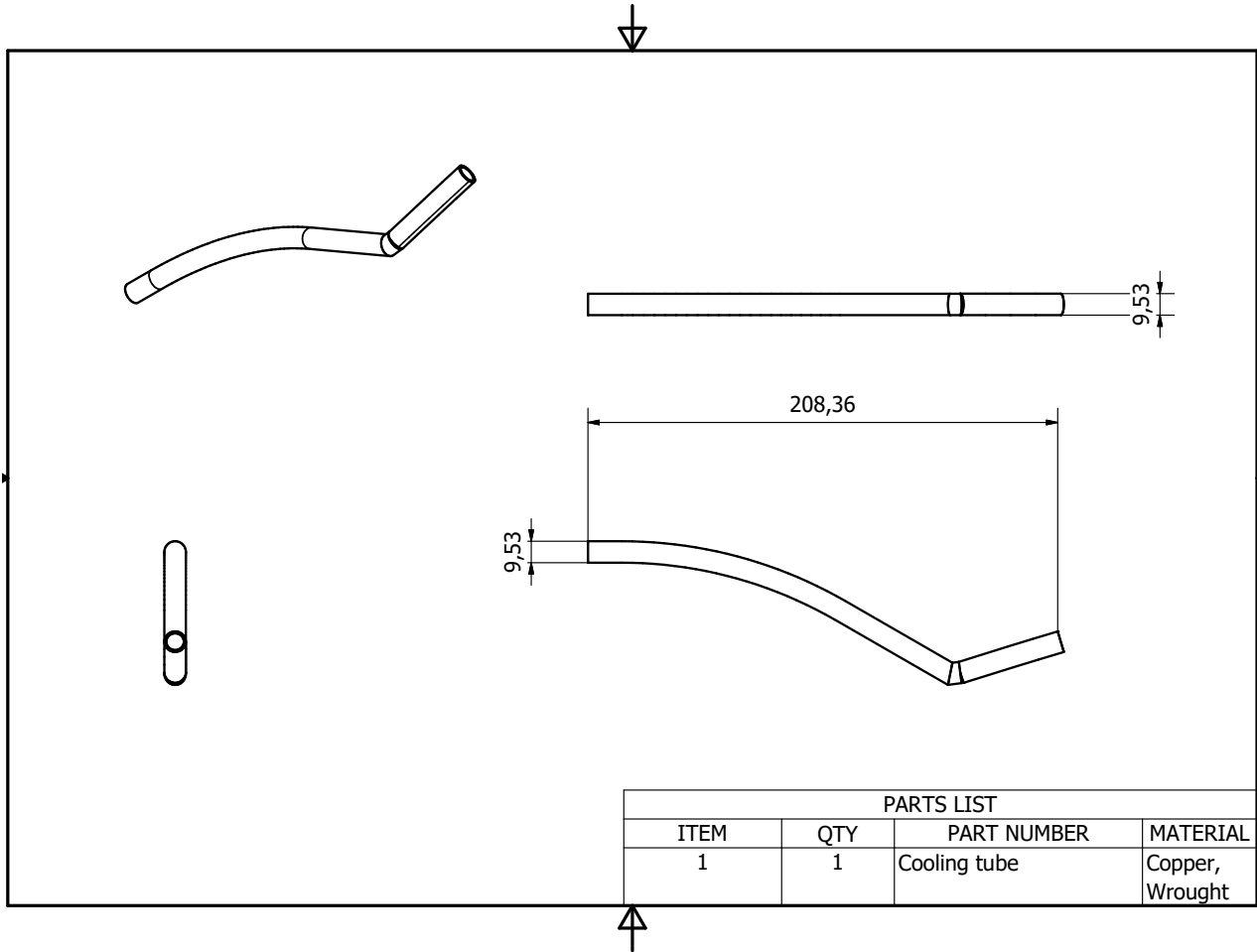


Figure 3.2.7: Cooling pipe geometry

hose and has to be distributed to the ten tubes. The manifold was integrated in to the outer wall of the combustion chamber. The outer wall of the cooling assembly was required to:

- Protect the cooling tubes from damage during clamping and static firing.
- Offer a structure to easily clamp the engine to the test stand frame
- Offer a way of cooling the engine through radiation

The material for the outer wall was chosen as stainless steel due to its high strength and relatively good thermal conductivity. The outer wall was designed as shown in Figure 3.2.8.

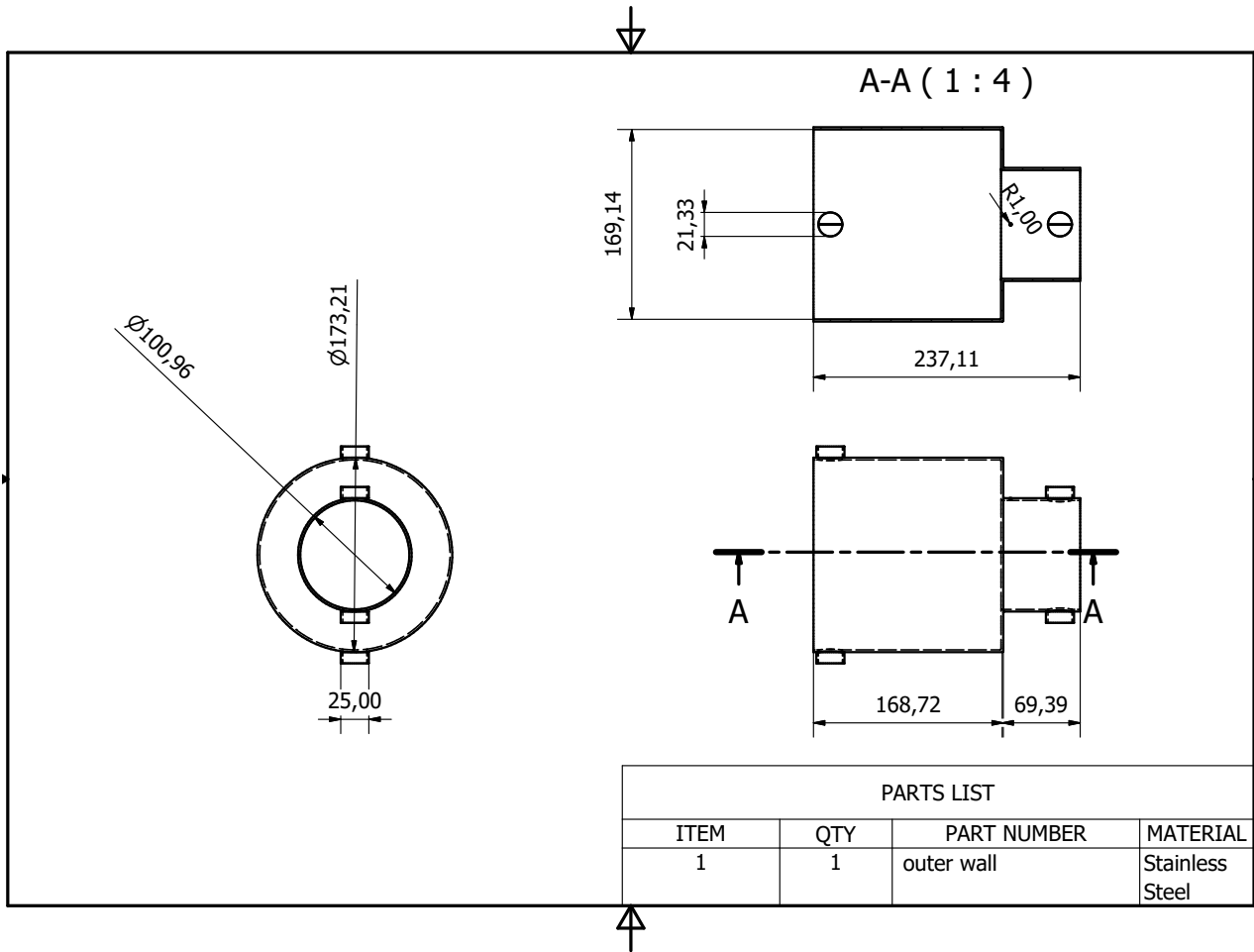


Figure 3.2.8: Outer wall part drawing

The outer wall was used to form part of the inlet and outlet manifold. The functional requirement of the manifolds is to supply fluid to the cooling pipes and to take away fluid from the cooling pipes. The manifold design was as shown below:

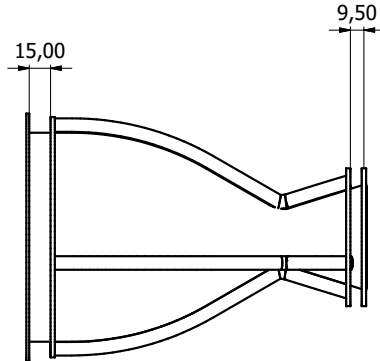


Figure 3.2.9: Cooling manifold design

(g) Data collection

The primary mode of data collection will be experimental testing after fabrication. This will provide the efficiency of the cooling system in real world conditions. The performance can however be estimated by the use of a mathematical model of the system. The developed cooling system was modelled and the heat transfer equations mentioned in section 2.4 used. This model, shown in Figure 3.2.10 was used to check if the wall temperature was kept within the acceptable range as well as confirming the effect of varying the flow rate on cooling. This model serves to provide theoretical values for dynamic cooling.

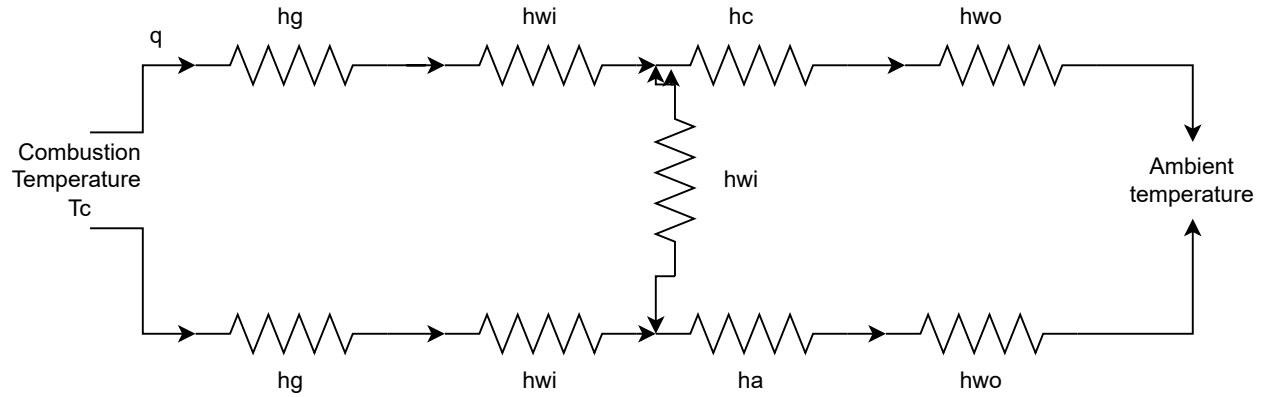


Figure 3.2.10: Cooling subsystem model

(h) Data analysis

Data analysis was done and is presented in the results section.

3.2.4 Coolant plumbing subsystem

The main aim of the coolant delivery subsystem is to deliver the coolant at high pressures and allow distribution into the cooling tubes. The subsystem is also responsible for collecting the spent coolant in the case of the test stand. The design of this subsystem was as follows:

1. Design requirements

The design requirements of the coolant plumbing subsystem can be described as

- Functional requirements
 - (a) The pump should be able to deliver the coolant to the channels at the required flow rate
 - (b) The subsystem should offer a way to integrate sensors for parameter measurement,

- (c) The subsystem should be able to achieve dynamic cooling by varying the flow rate of the pump.
- Non-functional requirements
 - (a) The subsystem should be easy to assemble.
 - (b) The subsystem should offer a fail safe mechanism.

2. Design considerations

The following were design considerations for the coolant plumbing subsystem:

- The mass flow rate of the coolant through the system.
- The sensors to be used to measure coolant properties.
- The size of the tubing used to deliver the coolant.
- The size of the pump in the system

3. Conceptual design

The design requirements and considerations led to development of one conceptual design. The conceptual design comprises of two reservoirs, a pump and the connecting tubes to and from the engine. The design is as shown below:

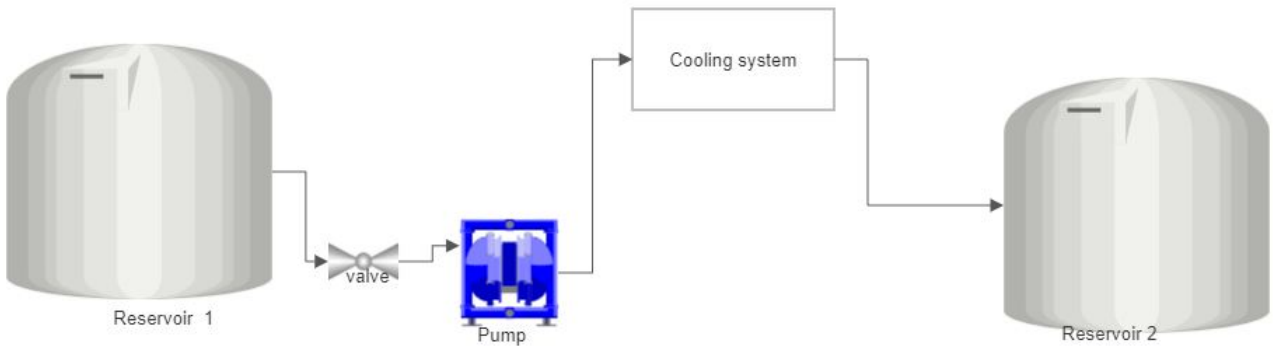


Figure 3.2.11: Piping system conceptual design

4. Tank selection The main considerations for the selection of the tank were the running time of the system and the need to incorporate sensors. The tank geometry was chosen to utilize readily available tanks. The calculations for tank geometry were as follows:

$$\text{Mass flow rate of coolant} = 0.5 \text{ kg/s}$$

$$\text{Proposed running time} = 5 \text{ minutes}$$

$$\begin{aligned} \text{Mass} &= 0.5 \text{ kg/s} \times 60 \times 3 \\ &= 90 \text{ kg} \end{aligned} \tag{3.2.4}$$

$$\text{Density of ethanol} = 789 \text{ kg/m}^3$$

$$\begin{aligned} \text{volume} &= \frac{\text{mass}}{\text{density}} \\ &= \frac{90 \text{ kg}}{789 \text{ kg/m}^3} \\ &= 0.114 \text{ m}^3 \\ &\approx 0.12 \text{ m}^3 \end{aligned} \tag{3.2.5}$$

Thus two plastic tanks of capacity 120 liters were selected shown in Figure 3.2.12.



Figure 3.2.12: 120l Plastic tank

5. Tube design

The tubes to be used were designed according to the mass flow rate of the fuel. The value of the diameter was obtained from another team working under the Nakuja Project.

6. Plumbing design

The plumbing for cooling purposes was done as shown in figure 3.2.13

7. Data collection

Data collection for the subsystem includes the modelling of the flow to ensure the required pressure and mass flow rate are achieved. The modelling also includes parameters for dynamic cooling.

8. Data analysis

The data obtained was analysed and is presented in the results section.

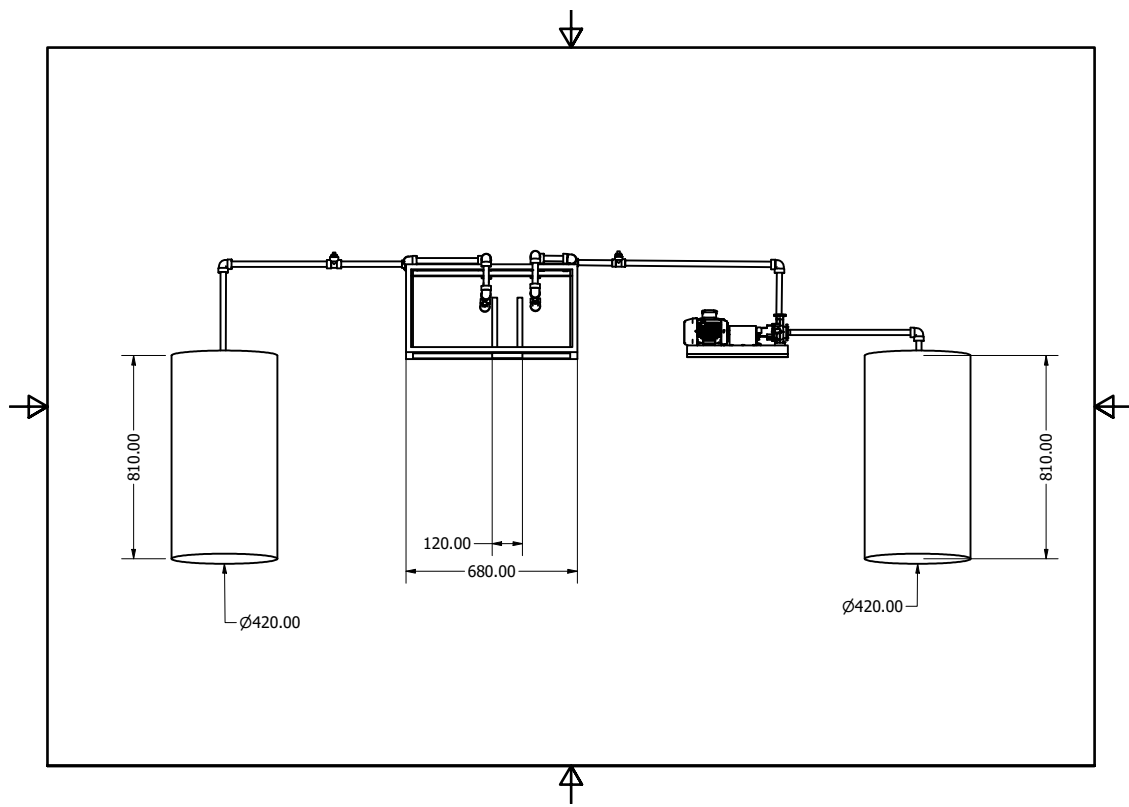


Figure 3.2.13: Plumbing for cooling

3.3 Electrical Module

The electrical module design is expected to provide electrical power to various electrical components throughout the project. This design will also facilitate transmission of electrical signals between the components. The components to be powered are a microcontroller unit which is an NodeMCU ESP32 board, sensors and an actuator in the form of a pump. The module allows the microcontroller unit to get data from the sensors. It also allows for the transmission of control signals from the microcontroller to the actuator.

3.3.1 Design requirements

1. Functional Requirements
 - (a) Appropriate power should be delivered to the pump in order to pump the fluid through the plumbing system effectively.
 - (b) The module should facilitate variation of power delivered to the pump.
 - (c) The electrical module should allow for an interface to receive user inputs and display outputs to the user.
 - (d) The electrical module should allow for delivering of appropriate power to the microcontroller and sensor suite.
 - (e) The electrical module should allow for powering and control of a heater in order to facilitate for testing of the cooling system.
2. Non-functional requirements
 - (a) Power efficiency.
 - (b) Safety.
 - (c) Minimum heat dissipated.
 - (d) Aesthetically pleasing connections.

3.3.2 Pump selection

The considerations were:

1. Flow rate

The base mass flow rate of the fuel and therefore coolant is 0.5161kg/s. This in cubic metres per hour is shown in equation 3.3.1 below.

$$\begin{aligned}
 volume &= \frac{mass\,flow\,rate}{density} \\
 &= \frac{0.5161\,kg/s}{789\,kg/m^3} \\
 &= 6.542 * 10^{-4} m^3/s \\
 &= 2.355 m^3/hr
 \end{aligned} \tag{3.3.1}$$

2. Viscosity of the fluid

Highly viscous fluids are more suited to positive displacement pumps while fluids with low viscosity like fresh water are more suited to centrifugal pumps.

3.3.3 Conceptual design

The conceptual design comprises of:

1. Power Distribution Circuit

The design considerations include:

- (a) Should avail appropriate power in terms of voltage and current to each of the components from the main power supply.
- (b) Incorporate safety features to prevent damage to the components.
- (c) Design should protect from electrical noise to ensure the signal integrity is maintained throughout the circuit.

- (d) Allow for manual overrides to the system in the event of a power emergency

2. Pump circuitry

The design requirements include:

- (a) Should provide 2700W maximum power to pump the cooling fluid at the desired variable rates from 2.355 cubic metres per hour, the fuel base flow rate to 7 cubic metres per hour which is the maximum flow rate achievable by the pump.
- (b) Should fit well into the mechanical structure.

3. Sensors

These sensors are as follows:

- (a) Temperature sensors
- (b) Pressure sensors

The design considerations will be:

- (a) The sensors should provide accurate and consistent data.
- (b) The sensors should be compatible with the chosen microcontroller.
- (c) Temperature sensors should achieve the required range from 24 °C to 1300 °C.

4. Display panel.

The display panel should appropriately and promptly relay communication from the system to the user.

3.3.4 Implementation of the design

1. Power Distribution

Appropriate power is delivered to the microcontroller, sensors, LCD interface and to the pump. AC power through the mains is rectified to DC power to power

the microcontroller and the sensors. The power distribution schematic is shown in Figure 3.3.1 below.

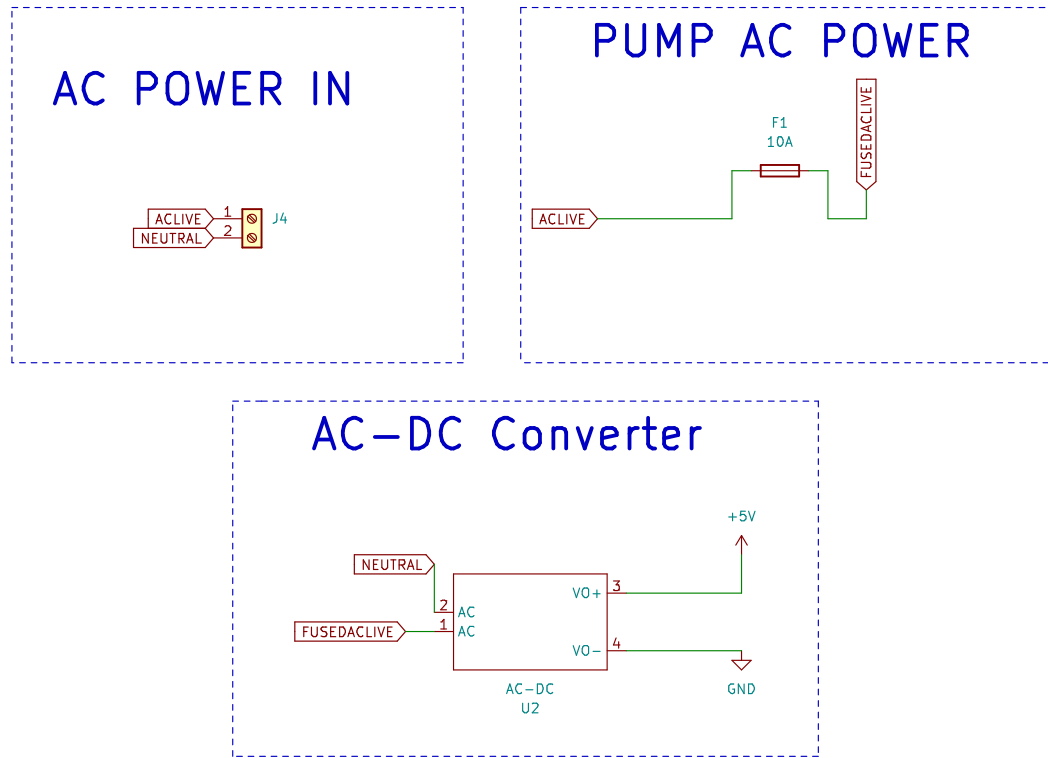


Figure 3.3.1: Power distribution

2. Pump circuitry

The pump circuitry allows for provision of power at variable rates to the pump. A Triac is used for switching purposes. A PWM signal from the microcontroller through an optocoupler for isolation purposes. The pump circuit schematic is as shown in Figure 3.3.2.

3. Heater Circuit

The heater circuit allows for turning on and off of the heater using commands from the microcontroller. As the heater is used for testing purposes, the above is a safety

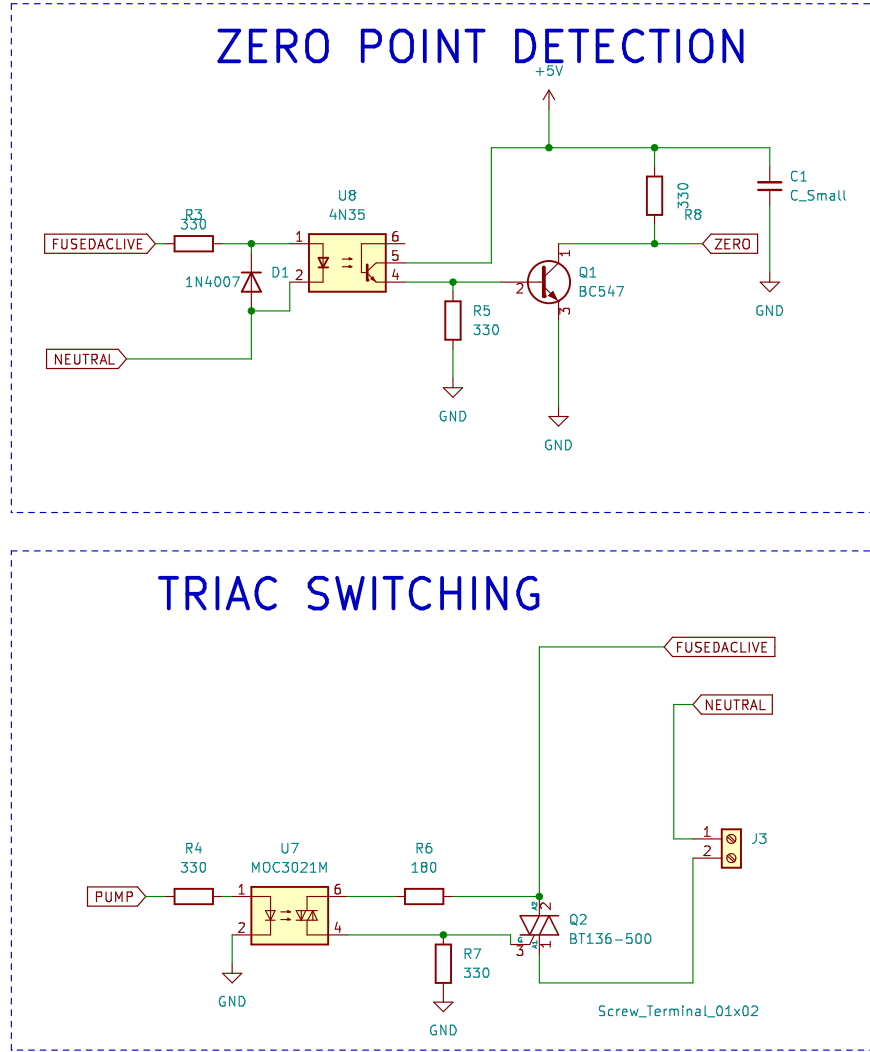


Figure 3.3.2: Pump circuitry

measure in the event of an anomaly in the sensor data.

3.3.5 Data collection

This was achieved through modelling and simulation. The electrical system was modelled using an electrical modelling software known as proteus. This was to primarily check

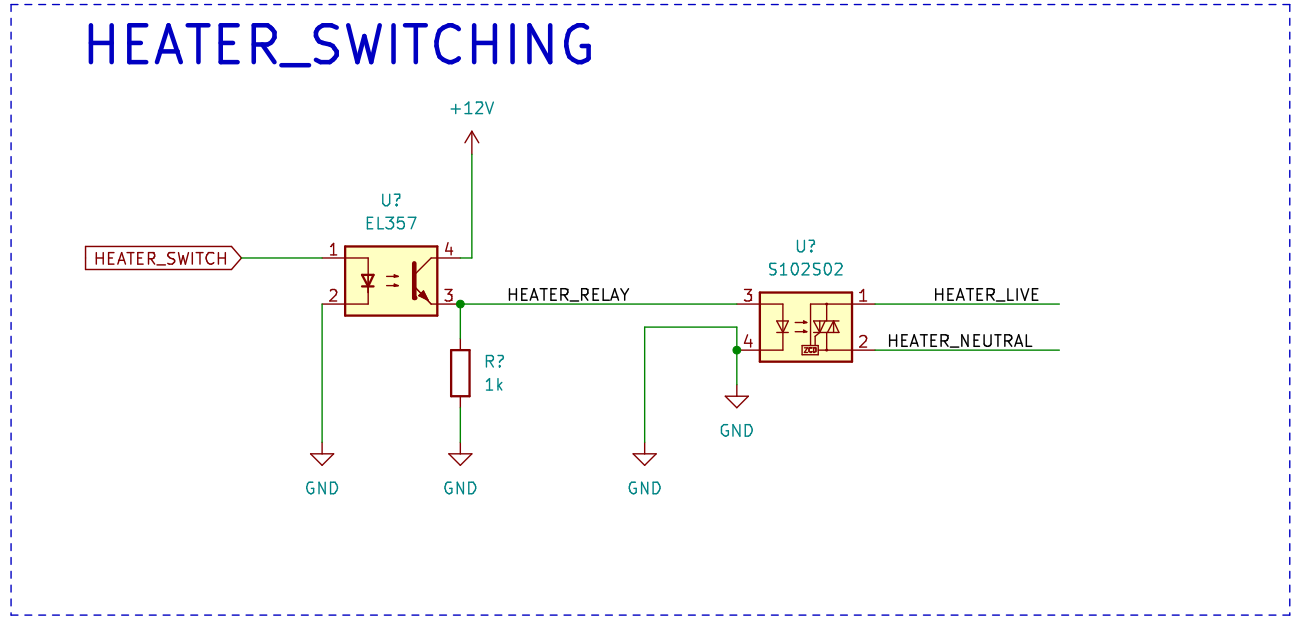


Figure 3.3.3: Heater circuit

whether the circuit achieves the primary objective of providing sufficient power safely.

The data collected from the simulation software included:

1. Voltage drop at each component.

The simulation also allowed for testing of the circuit to deliver variable AC power as shown in Fig 3.3.4

3.3.6 Data analysis

This is analysis of the data collected from carrying out simulations. The voltage data was used to determine:

1. Control parameters of power delivered to the pump.

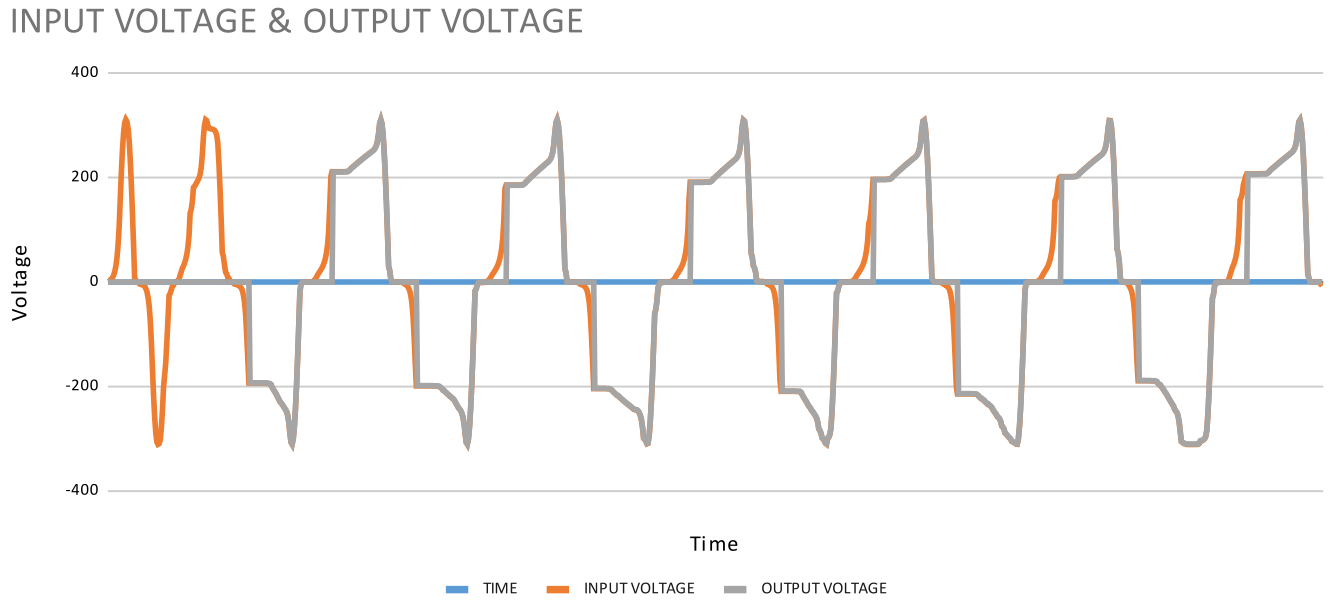


Figure 3.3.4: Power control.

2. Amount of power consumed by the proposed solution.
3. Signal processing required on the data acquired from the sensors.

3.4 Control module

3.4.1 Design requirements

1. Functional requirements
 - (a) The module is designed to take temperature sensor data as input.
 - (b) The control module is designed to determine the actuation required from the temperature sensor data which depicts the current state of the system.
 - (c) The control module design allows for provision of appropriate signals to the pump to allow for appropriate actuation.

2. Non-functional requirements.

The algorithm designed is straightforward and will allow for direct implementation.

3.4.2 Control algorithm

The control algorithm is meant to achieve dynamic cooling. This is done by varying the mass flow rate of the pump supplying coolant to the coolant tubes. The heat flux is dependant on the thermal co-efficient of the liquid coolant shown by equation 2.4.8 and 2.4.9. The thermal co-efficient of the coolant denoted as h_l is directly proportional to the Nusselt number. The Nusselt number varies with the Reynolds Number which is affected by the coolant velocity. Thus the expression for h_l can be simplified as:

$$h_l = kRe^{0.8} \quad (3.4.1)$$

where

k = constant for the system as all the other parameters of the Nusselt number are constant at constant coolant temperature and pressure.

Re = Reynolds number

The equation for Reynolds number can be further simplified as

$$Re = kv \quad (3.4.2)$$

where k = represents the time invariant constants

v = velocity of the coolant in the cooling channels.

Thus the equation for the thermal co-efficient for the coolant liquid film can be rewritten as:

$$h_l = kv^0.8 \quad (3.4.3)$$

where

k = constant at constant coolant temperature and pressure

v =velocity of the coolant in the cooling channels

The heat flux can be obtained by measuring the temperature change of the coolant hence according to equation 2.4.8 and 2.4.9 the thermal co-efficient and the wall temperature can be controlled by controlling the mass flow rate of the coolant. The control algorithm is as shown in figure 3.4.1 below.

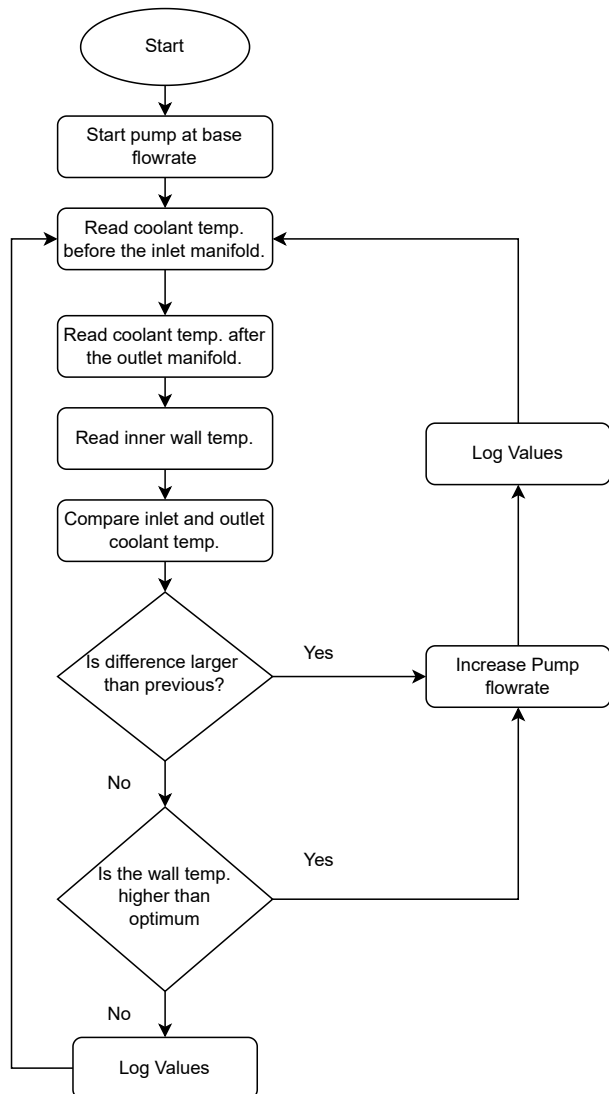


Figure 3.4.1: Program flow chart

3.4.3 Data collection

1. Modelling and simulation

The control algorithm will be modelled using computer software and different algo-

rithms simulated and responses observed. The data collected will be visualized to compare input signals and the responses that consequently occur.

2. Experimental testing The fabricated mechanism will undergo iterative testing to acquire the optimum tuning parameters of the control algorithm. Table 3.4.1 shows the inputs and outputs for the system.

Table 3.4.1: Experimental data outputs and outputs

Inputs	Outputs
Coolant temperature	wall temperature
Pump power	coolant flow rate
	Pressure drop

The data collected will be relayed to a dashboard and stored.

3.4.4 Data analysis

The data from simulation will be used to design a PID controller for the system. This will then be actualized through firmware to be run on the system's microcontroller.

Chapter 4

Results

The results are grouped according to the mechanical,electrical and control system.

4.1 Mechanical module

The design process yielded a rocket engine nozzle designed for regenerative cooling as well as the supporting structure. Crucially the design was also analysed using numerical means to ensure that it met minimum design specifications, performance and safety parameters. The results of fluid flow analysis, thermo-structural analysis and heat transfer analysis are presented in this section.

4.1.1 Cooling system design

The engine assembly is as shown in Figure 4.1.1.

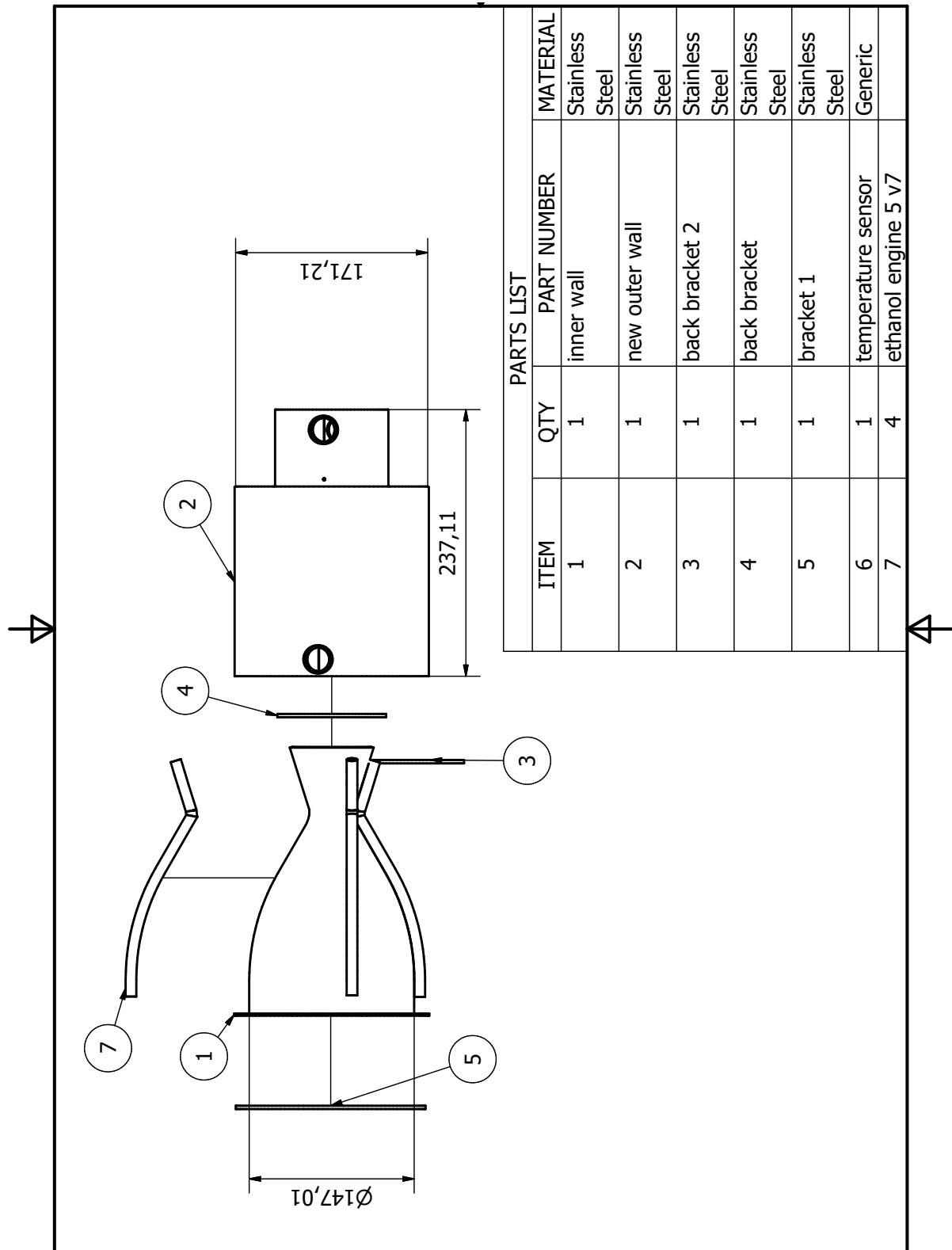


Figure 4.1.1: Liquid engine geometry



Figure 4.1.2: 3D Engine assembly

The 3D view is shown in Figure 4.1.2.

The completed assembly including the cooling system is as shown in figure

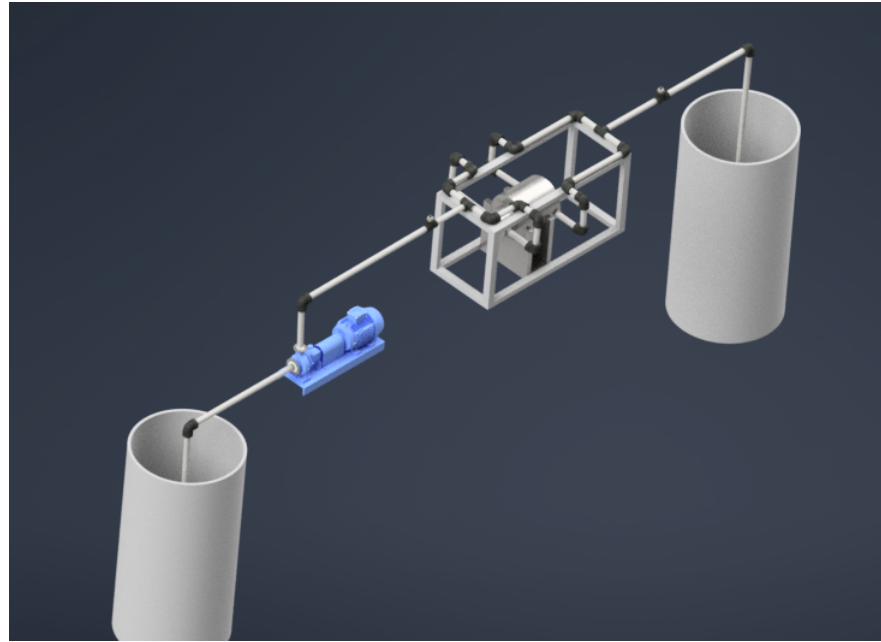


Figure 4.1.3: Completed mechanical assembly

4.1.2 Design validation

Fluid flow analysis

The boundary conditions used:

Table 4.1.1: Boundary conditions fluid flow analysis

General setting	Density-based Analysis Energy-On
Solver	k-e Epsilon
Solution type	Second order Upwind
Pressure	2 Mpa
Temperature	3232K

The result are as shown:

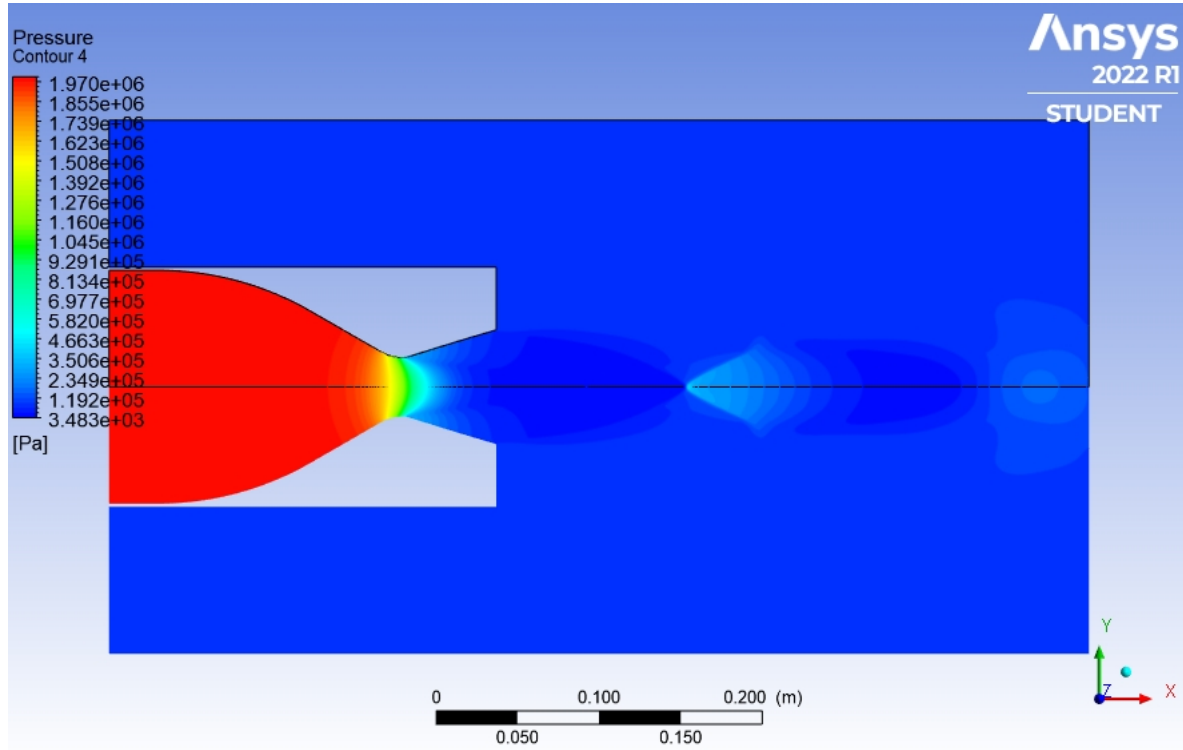


Figure 4.1.4: Fluid flow analysis- Pressure

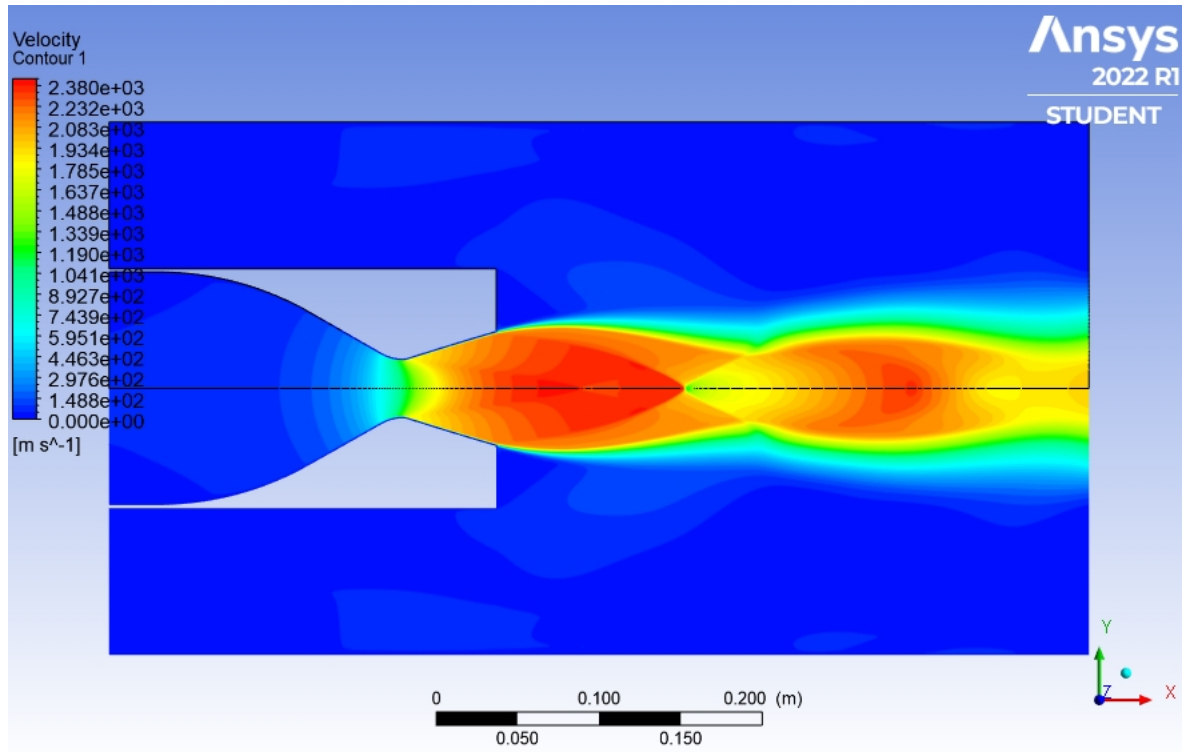


Figure 4.1.5: Fluid flow analysis- Velocity

From the images above the following can be deduced:

- The exit pressure(119200) is higher than ambient pressure meaning that the flow is under-expanded. This is desired so as to eliminate issues with over-expansion such as flow separation.
- The velocity at the throat is equal to Mach 1 which is desirable.
- The velocity and pressure images do not show any shock waves.
- The exit velocity is higher than Mach 1.

Thus the designed geometry meets the required specifications.

Thermo-structural analysis

The boundary conditions used:

Table 4.1.2: Boundary conditions fluid flow analysis

General setting	Density-based Analysis Energy-On
Solver	k-e Epsilon
Solution type	Second order Upwind
Pressure	2 Mpa
Temperature	3232K
Material	Stainless steel
Wall thickness	2mm

The results are shown:

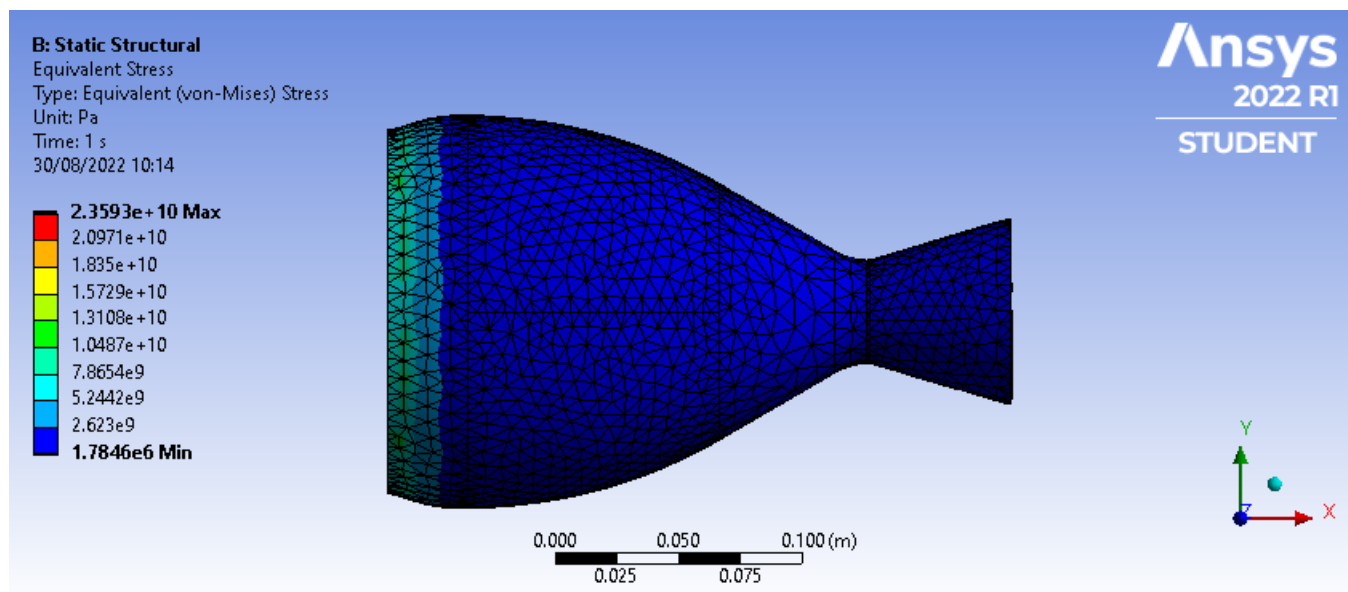


Figure 4.1.6: Thermo-structural analysis- Stress analysis

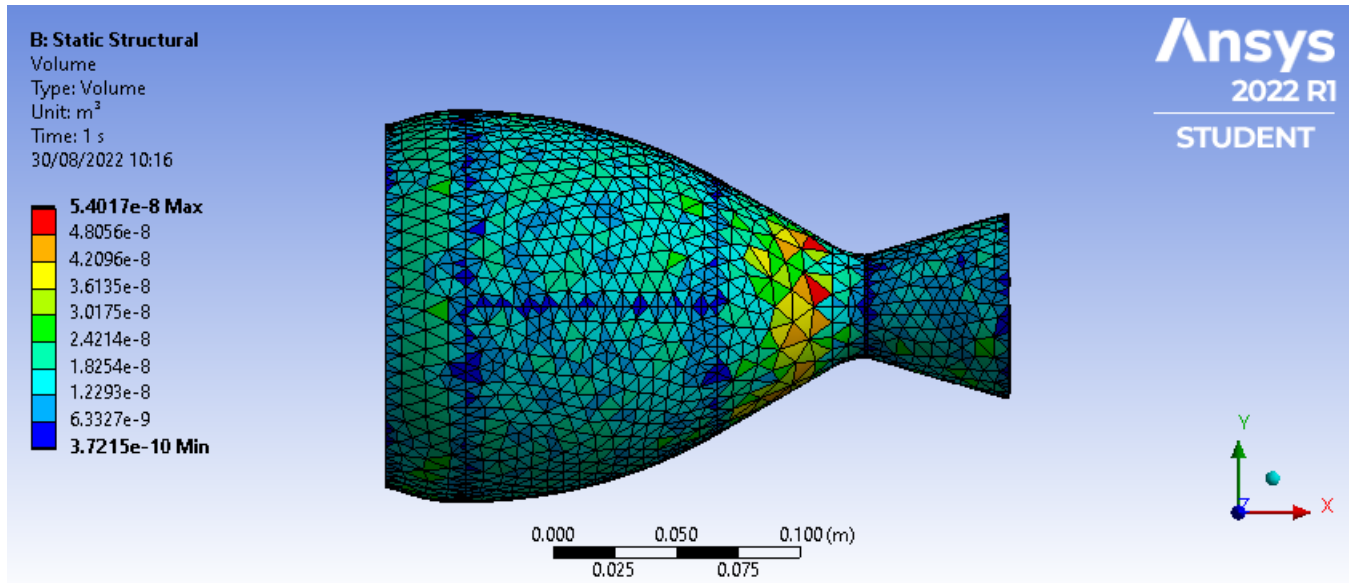


Figure 4.1.7: Thermo-structural analysis- Volumetric analysis

From the analysis it can be concluded that:

- The stresses experienced are within the acceptable ranges
- The chosen thickness is sufficient for engine performance.

Heat transfer analysis

The heat transfer equations were used to determine the temperature of the wall and how effective the proposed cooling system is. RPA software was used to determine the temperature of the uncooled chamber shown in Figure 4.1.8.

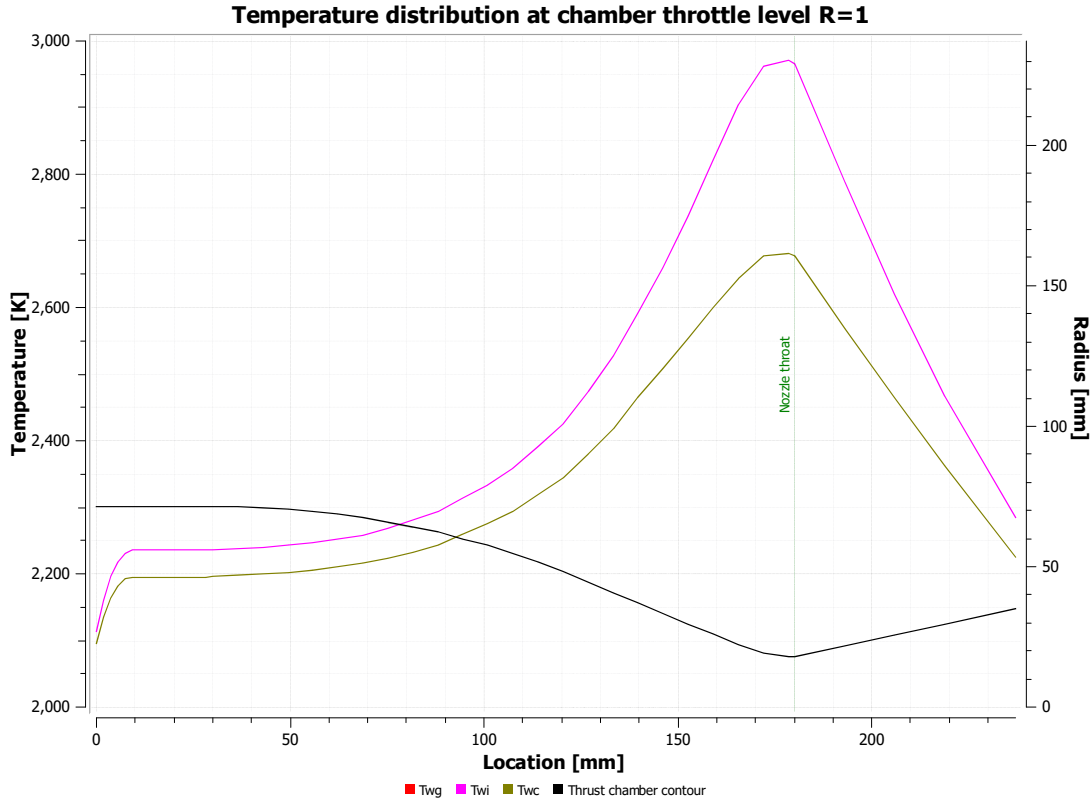


Figure 4.1.8: Uncooled wall temperature

From Figure 4.1.8 it can be seen that the wall temperature exceeds the melting point of Grade 304 Stainless steel which is 1673K or 1400 °C. The model generated of the proposed cooling system was solved using the heat transfer equations listed in section 2.4. As dictated by the model shown by Figure 3.2.10 the first step was to calculate the gas film co-efficient H_g . The next co-efficient to be calculated were the conduction co-efficient of the wall of the chamber and that of the wall of the cooling tube. The film co-efficient was then calculated. All co-efficients were solved and the adiabatic gas temperature determined. This was used to determine the temperature of the wall. The model parameters are as listed in Table 4.1.3.

Table 4.1.3: Cooling system Model Parameters

Name	Value
Inner wall Material	Stainless steel Grade 304
Cooling tube geometry	circular d=9.525mm
Cooling tube material	wrought copper
Stainless steel thermal conductivity	16 W/mK
Wrought copper	320 W/mK
Wall thickness	2 mm
Coolant	Ethanol
Minimum coolant flow rate	0.52 kg.s

The model was solved and yielded the following results:

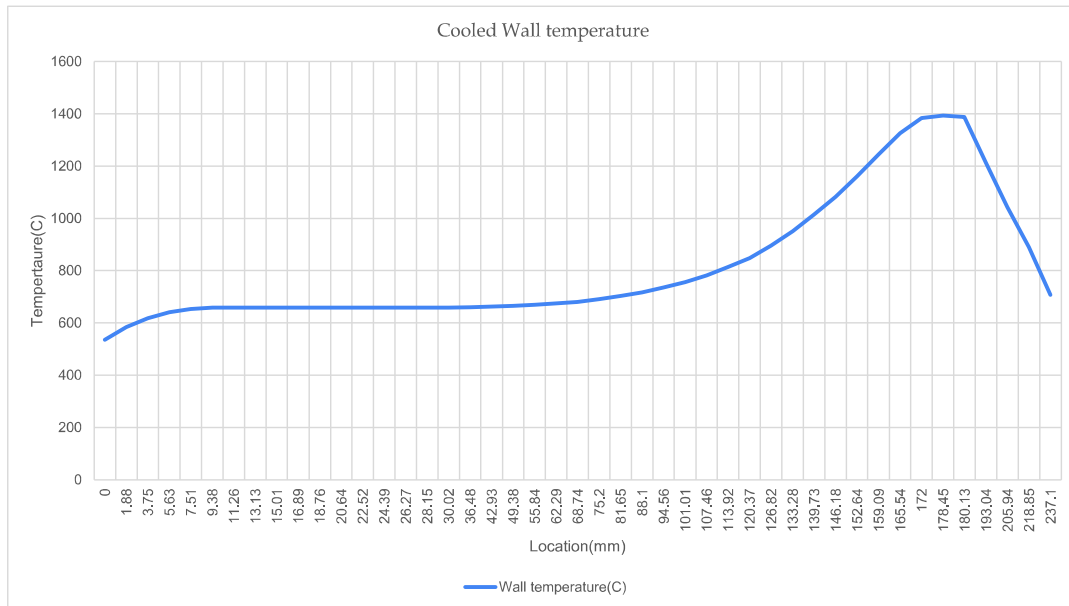


Figure 4.1.9: Wall temperature-cooled

From figure 4.1.9 it is shown that the cooled wall temperature is just below the melting point of steel which is 1400 °C. The cooling was done at a mass flow rate of 0.5Kgs. This shows that the cooling system achieves cooling and investigation of higher coolant velocities is required to determine the most appropriate mass flow rate for optimum operation. It is proposed that the wall is required to be kept below 1000°C.

4.2 Electrical module

During the design of the electrical module, a power budget was determined based on the individual components characteristics. The power budget is as shown in table 4.2.1.

Table 4.2.1: Power budget

Component	Voltage(V)	Current(A)	Power(W)	Number of components	Duty Cycle	Total power(W)
Pressure sensor	5	0.02	0.1	2	1	0.2
MLX90614	3.3	0.02	0.066	1	1	0.06
DSB1820	3.3	0.02	0.066	2	1	0.132
LCD Screen	5	0.16	0.8	1	1	0.8
ESP32	3.3	0.5	1.65	1	1	1.65
Heater	240	11.25	2700	1	1	2700
Pump	240	5.2	1248	1	1	1248
Total						3950.842

The electrical module design was culminated in a printed circuit board. The board design allows for powering of components and transmission of signals between various components. The circuit board is shown in figure 4.2.1.

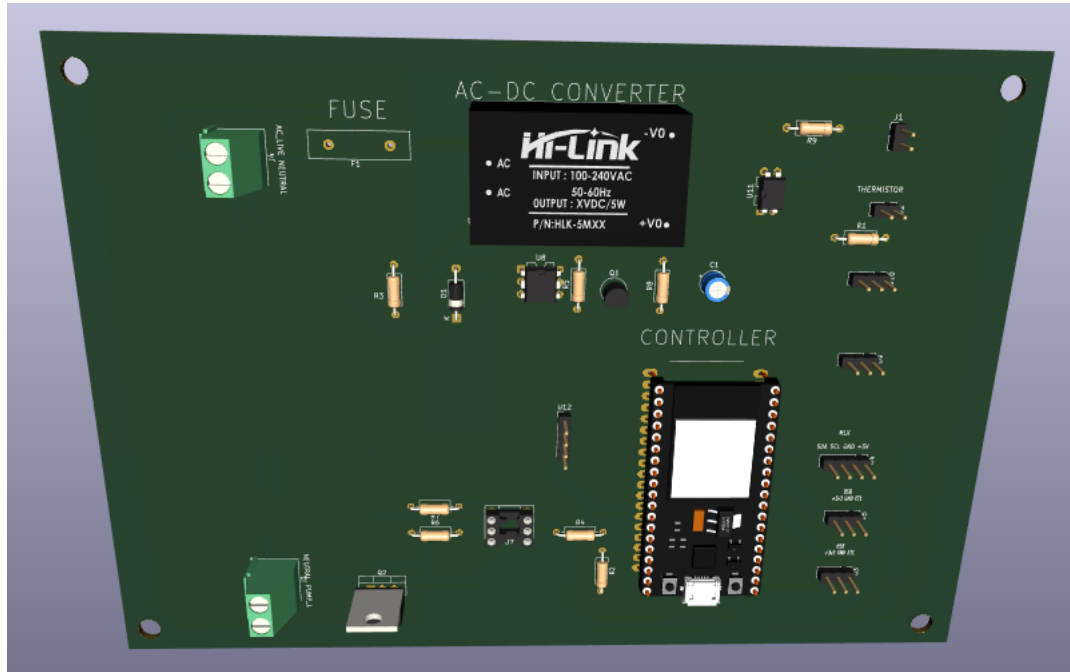


Figure 4.2.1: Electronic design

4.3 Control module

The Human Interface for system was developed and is as shown in Figure 4.3.1.

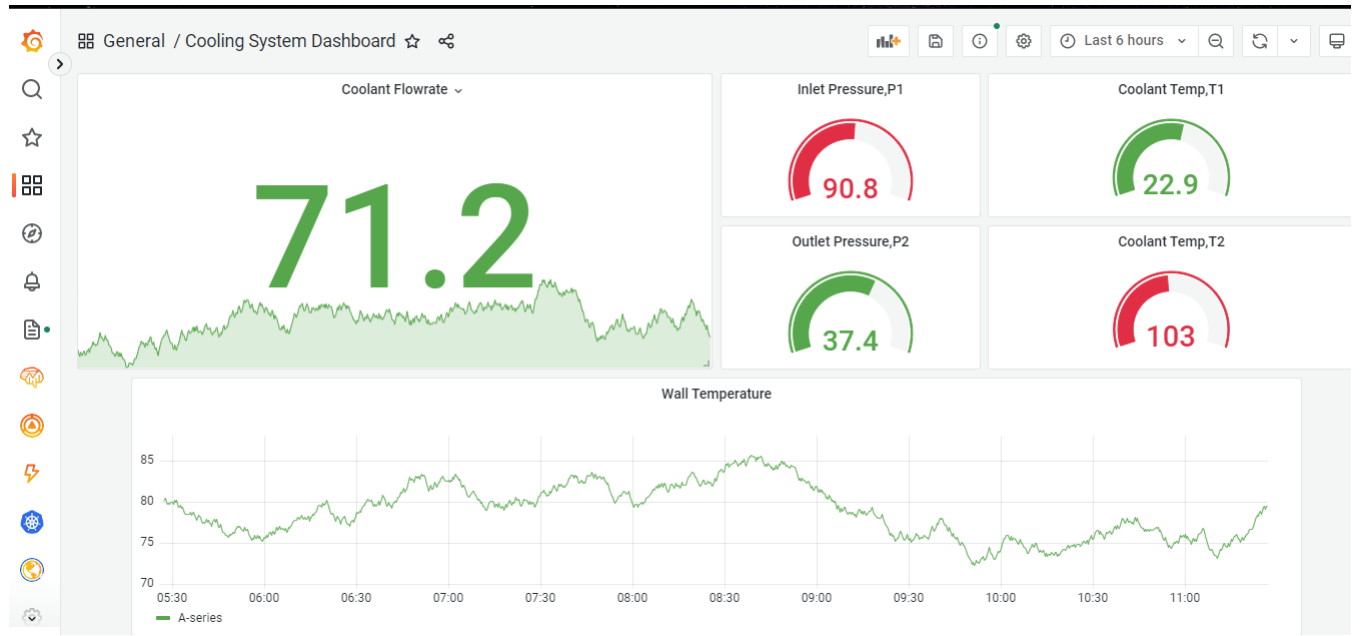


Figure 4.3.1: Human interface

Chapter 5

Conclusion

A liquid rocket engine with a thrust of 2.7kN and chamber pressure of 2MPa was designed. The liquid rocket engine was equipped with a regenerative cooling system. A test stand for the liquid rocket engine was designed to test the efficiency of the cooling system without the need for static testing.

The design of the liquid rocket engine was validated by fluid flow analysis using ANSYS software. Thermo-structural analysis was also conducted to determine mechanical stresses. The design was found to sufficiently hold the expected loads.

A heat transfer analysis was conducted on the designed engine to determine the temperature of the engine and heat fluxes expected during operation. A model of the designed cooling system was developed and calculation conducted to evaluate performance. A relationship between mass flow rate of the coolant and the wall temperature was identified and used to develop a method for dynamic cooling. The model of the cooling system was solved with minimum mass flow rate to identify cooling capacity and the results presented.

Bibliography

- [1] D. K. Huzel and D. H. Huang, *Design of Liquid Propellant Rocket Engines*, Scientific and Technical Information Office, National Aeronautics and Space Administration [Online]. Available, 1967. [Online]. Available: <https://books.google.co.ke/books?id=UpqgnQEACAAJ>
- [2] O. B. George P. Sutton, *Rocket Propulsion Elements*, 9th ed. Wiley, 2016. [Online]. Available: libgen.li/file.php?md5=baee518e4f11a10b9506b7b66d7632c1
- [3] E. A. Santos, W. F. Alves, A. N. A. Prado, and C. A. Martins, “Development of test stand for experimental investigation of chemical and physical phenomena in liquid rocket engine,” *Journal of Aerospace Technology and Management*, vol. 3, no. 2, pp. 159–170, 2011.
- [4] T. Vinitha, S. Senthilkumar, and K. Manikandan, “Thermal Design And Analysis Of Regeneratively Cooled Thrust Chamber Of Cryogenic Rocket Engine,” *International Journal of Engineering Research*, vol. 2, no. 6, p. 8, 2013.
- [5] S. H. Youngblood, “Design and Testing of a Liquid Nitrous Oxide and Ethanol Fueled Rocket Engine,” p. 222.
- [6] J. Hansen, “Student design of a bipropellant liquid rocket engine and associated infrastructure,” vol. 36.
- [7] T. P. G. Jr, “Heating and regenerative cooling model for a rotating detonation engine designed for upper stage performance,” p. 212.

- [8] J. Poulopoulos and T. Chronopoulos, “Cooling Methods in Combustion Chambers and Nozzles,” p. 40.
- [9] S. R. Shine and S. S. Nidhi, “Review on film cooling of liquid rocket engines,” *Propulsion and Power Research*, vol. 7, no. 1, pp. 1–18, 2018.
- [10] N. A. Adams, W. Schröder, R. Radespiel, O. J. Haidn, T. Sattelmayer, C. Stemmer, and B. Weigand, Eds., *Future Space-Transport-System Components under High Thermal and Mechanical Loads: Results from the DFG Collaborative Research Center TRR40*, ser. Notes on Numerical Fluid Mechanics and Multidisciplinary Design. Cham: Springer International Publishing, 2021, vol. 146. [Online]. Available: <http://link.springer.com/10.1007/978-3-030-53847-7>
- [11] R. C. Arnold, D. Suslov, and O. J. Haidn, “Experimental investigation of film cooling with tangential slot injection in a lox/ch₄ subscale rocket combustion chamber,” *Transactions of The Japan Society for Aeronautical and Space Sciences, Space Technology Japan*, vol. 7, 2009.
- [12] G. P. Richter and T. D. Smith, “Ablative material testing for low-pressure, low-cost rocket engines,” *presented at the Combustion Subcommittee, Propulsion Systems Hazards Subcommittee, Huntsville, AL, Oct*, vol. 1995, Jun. 2022. [Online]. Available: <https://ntrs.nasa.gov/citations/19960007443>
- [13] M. E. Boysan, “A thesis submitted to the graduate school of natural and applied sciences of middle east technical university,” vol. 100.
- [14] J. Haemisch, D. Suslov, G. Waxenegger-Wilfing, K. Dresia, and M. Oschwald, “LUMEN – DESIGN OF THE REGENERATIVE COOLING SYSTEM FOR AN EXPANDER BLEED CYCLE ENGINE USING METHANE,” p. 10.
- [15] M. Pizzarelli, “Regenerative cooling of liquid rocket engine thrust chambers,” *Roma: Agenzia Spaziale Italiana*, 2017.

- [16] D. K. Huzel, *Modern Engineering for Design of Liquid-Propellant Rocket Engines*. AIAA, 1992.
- [17] W. Yang and B. Sun, “Numerical simulation of liquid film and regenerative cooling in a liquid rocket,” *Applied Thermal Engineering*, vol. 54, no. 2, pp. 460–469, May 2013. [Online]. Available: <https://linkinghub.elsevier.com/retrieve/pii/S1359431113001269>
- [18] A. Dhara, P. M. Kishan, and V. V. Kannah, “Design of Regenerative Cooled Cryogenic Rocket Engine,” vol. 29, no. 10, p. 19, 2020.
- [19] L. Denies, “Regenerative cooling analysis of oxygen/methane rocket engines,” p. 143.
- [20] C. H. Marchi, F. Laroca, A. F. C. d. Silva, and J. N. Hinckel, “NUMERICAL SOLUTIONS OF FLOWS IN ROCKET ENGINES WITH REGENERATIVE COOLING,” *Numerical Heat Transfer, Part A: Applications*, vol. 45, no. 7, pp. 699–717, Apr. 2004. [Online]. Available: <http://www.tandfonline.com/doi/abs/10.1080/10407780490424307>
- [21] Y.-D. Kang and B. Sun, “Numerical Simulation of Liquid Rocket Engine Thrust Chamber Regenerative Cooling,” *Journal of Thermophysics and Heat Transfer*, vol. 25, no. 1, pp. 155–164, Jan. 2011. [Online]. Available: <https://arc.aiaa.org/doi/10.2514/1.47701>
- [22] F. V. Pelevin, N. I. Avraamov, N. Y. Ir’yanov, S. A. Orlin, V. V. Lozovetskii, and A. V. Ponomarev, “Intensification of Heat Exchange in the Regenerative Cooling System of a Liquid-Propellant Rocket Engine,” *Journal of Engineering Physics and Thermophysics*, vol. 91, no. 3, pp. 601–610, May 2018. [Online]. Available: <http://link.springer.com/10.1007/s10891-018-1781-4>
- [23] M. Murugesan and R. Balasubramanian, “The Effect of Mass Flow Rate on the Enhanced Heat Transfer Characteristics in A Corrugated Plate Type Heat Exchanger,” *Research Journal of Engineering Sciences*, vol. 1, no. 6, pp. 22–26, 2012.

- [Online]. Available: <http://www.isca.in/IJES/Archive/v1/i6/4.ISCA-RJEngS-2012-097.php>
- [24] B. Smith, “Materials for rocket construction - i,” *Astronautics*, vol. 5, no. 31, pp. 7–8, June 1935.
- [25] S. Shine and S. S. Nidhi, “Review on film cooling of liquid rocket engines,” *Propulsion and Power Research*, vol. 7, no. 1, pp. 1–18, 2018.
- [26] E. Andersson, “Preliminary design of a small-scale liquid-propellant rocket engine testing platform,” 2019.
- [27] “PROPELLANTS.” [Online]. Available: <https://history.nasa.gov/conghand/propelnt.htm>
- [28] A. Elsayed, R. K. AL-Dadah, S. Mahmoud, and W. Kaialy, “Investigation of Activated Carbon / Ethanol for Low Temperature Adsorption Cooling,” p. 40.

Appendices

Appendix A

Part drawings

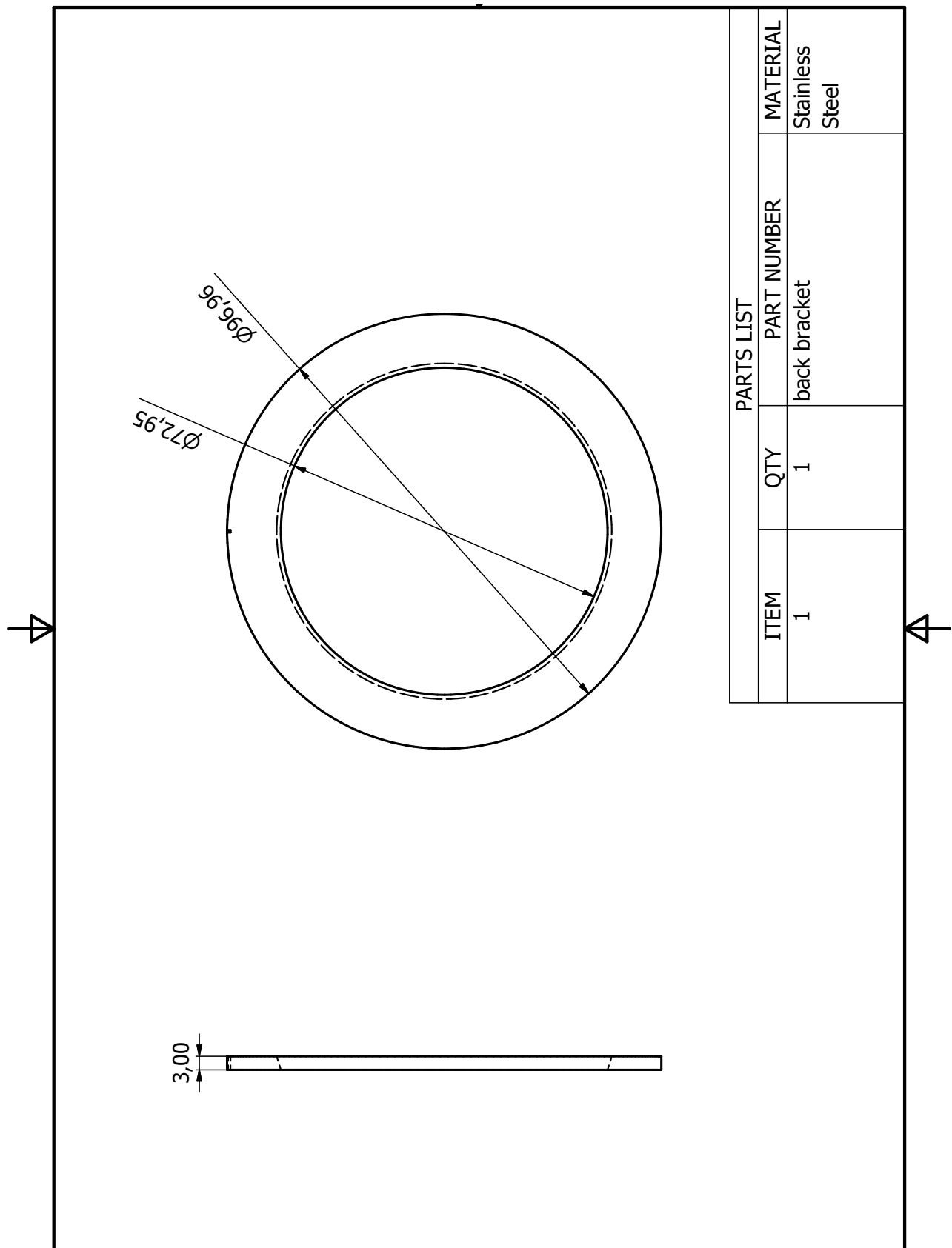


Figure A.0.1: Back bracket

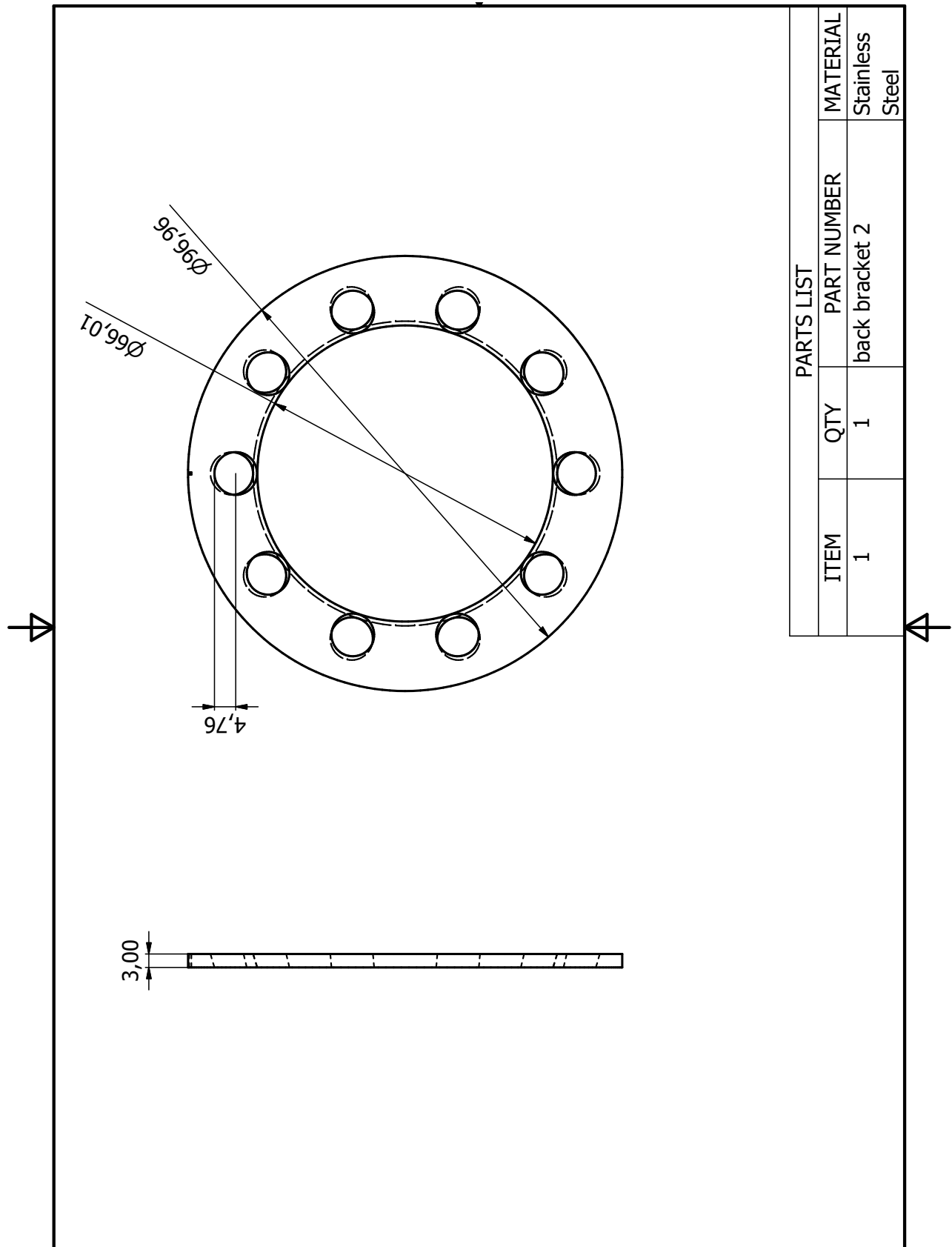


Figure A.0.2: Back bracket-2

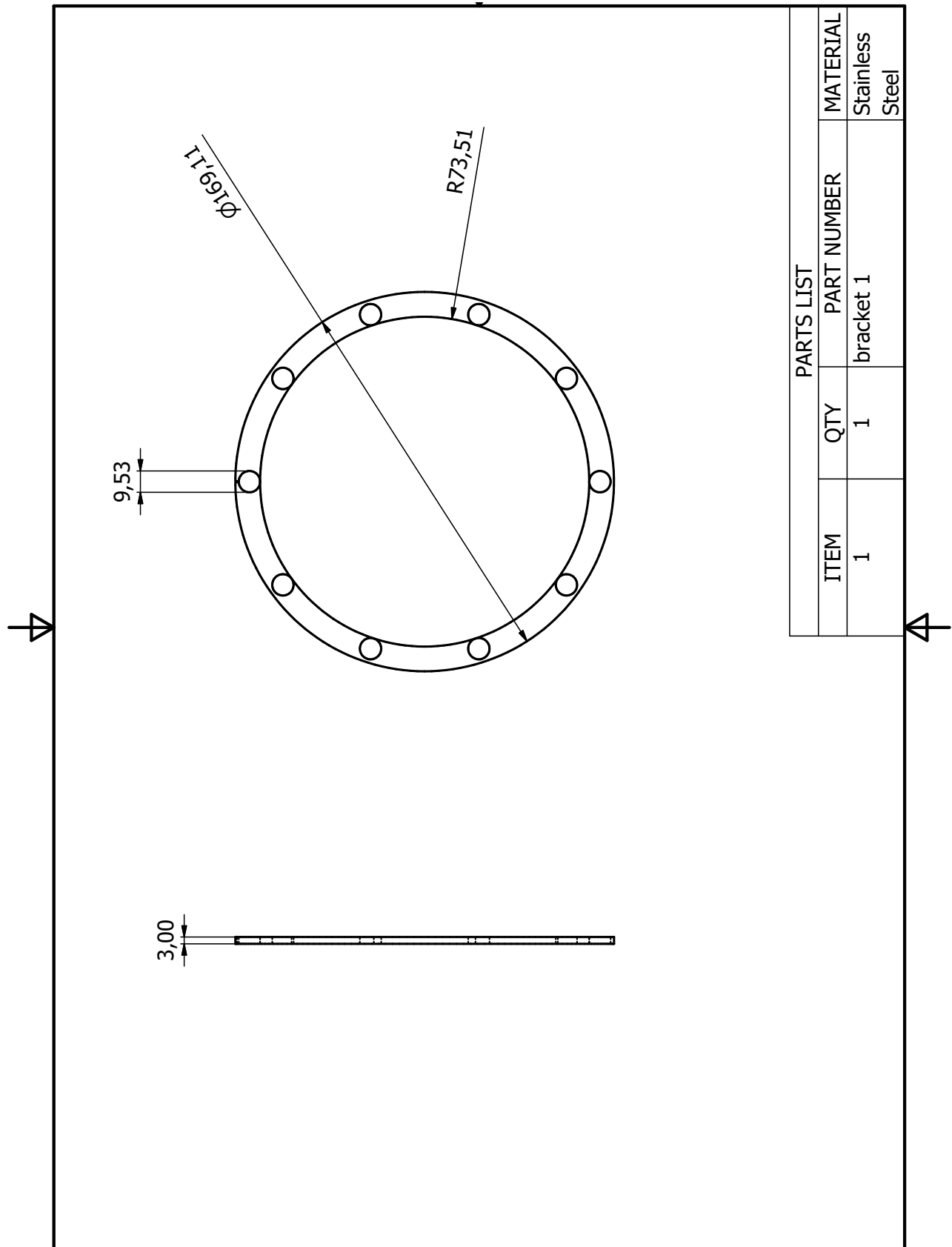


Figure A.0.3: Bracket-1

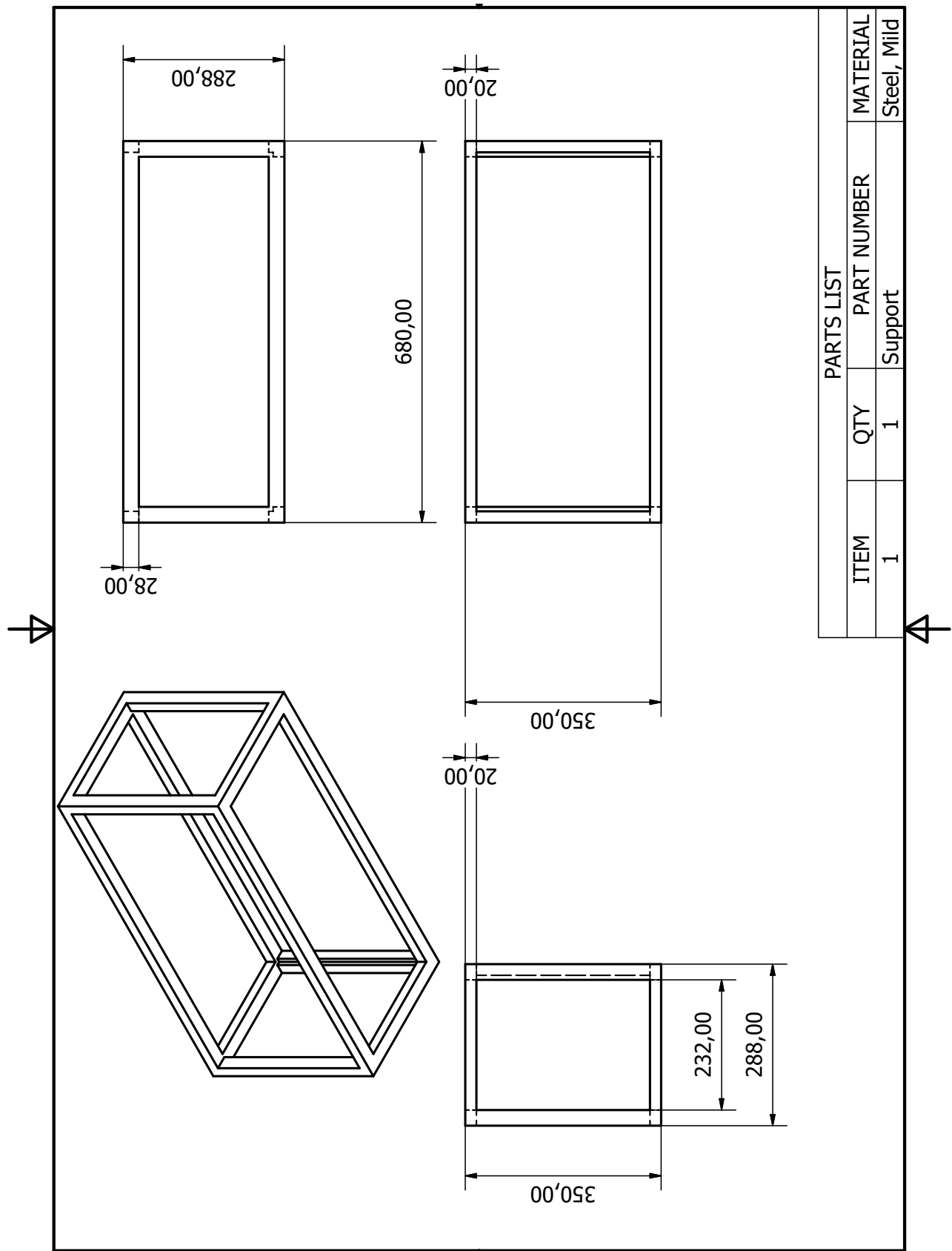


Figure A.0.4: outer shell

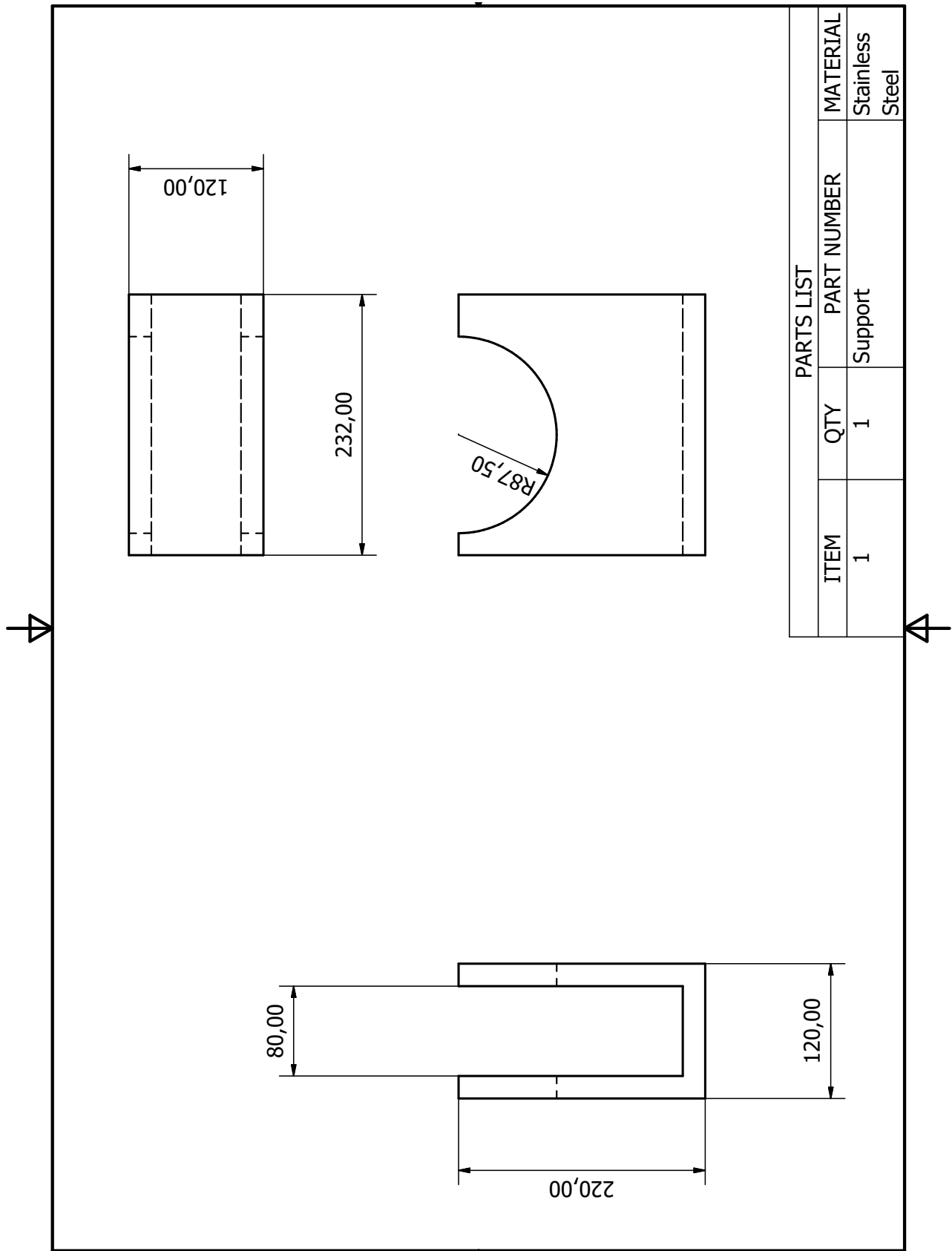


Figure A.0.5: Support

Appendix B

Budget and timeplan

B.1 Provisional budget

Item	Cost per unit (KShs)	Number of components	Total Cost
Pump	13500	1	13500
Plumbing fittings	2000	1	2000
Microcontroller(ESP32)	1400	1	1400
Assorted electronics	3000	1	3000
Pressure sensors	3000	2	6000
Stainless Steel(180mm diameter billet 18metres)	930	1	930
Temperature sensors	300	4	1200
Thermocouple	750	2	1500
Flow meter	1400	1	1400
Temperature sensors	300	4	1200
Tanks	735	1	735
Mild steel(250*20*230)	880	3	2640
Total			35505

Table B.1.1: Budget

B.2 Timeplan

Week	1	2	3	4	5	6	7	8	9	10	11	12	13	14	15	16	17	18	19	20	21	22	23	24	25	26	
Proposal Presentation	■	■																									
Literature Review	■	■	■	■	■	■	■	■	■	■	■	■	■	■	■	■	■	■	■	■	■	■	■	■			
Mechanical design			■	■	■	■	■	■	■	■	■																
Electrical and control design								■	■	■	■																
Continuous Presentation			■	■	■	■	■	■	■	■	■																
Interim report							■	■	■	■	■																
Mechanical fabrication												■	■	■	■	■	■	■	■	■	■	■					
Fabrication of electrical components and assembly																		■	■	■	■	■	■	■	■		
Control algorithm implementation																					■	■	■	■	■		
Assembly and testing																					■	■	■	■	■		
Final Presentation																								■	■	■	

Table B.2.1: Time plan

Appendix C

Programming Code

C.1 CEA output parser-Python code

```
import matplotlib.pyplot as plt
import pandas as pd
import numpy as np
import os
import sys

def annot_max(x,y, ax=None):
    xmax = x[np.argmax(y)]
    ymax = y.max()
    text= "x={:.3f}, y={:.3f}".format(xmax, ymax)
    if not ax:
        ax=plt.gca()
    bbox_props = dict(boxstyle="square,pad=0.3", fc="w", ec="k", lw=0.72)
    arrowprops=dict(arrowstyle="->",connectionstyle="angle,angleA=0,angleB=60")
```

```
kw = dict(xycoords='data',textcoords="axes fraction",
          arrowprops=arrowprops, bbox=bbox_props, ha="right", va="top")
ax.annotate(text, xy=(xmax, ymax), xytext=(0.94,0.96), **kw)

file_name = input("Please input the file name:\n")
fuel_name = input("Please input the name of the fuel:\n")
file = open(os.path.join(sys.path[0],file_name)).read()
outputs = file.split('THEORETICAL')
outputs = outputs[1:]
df = pd.DataFrame()
Of_ratio = []
Imp = []
Kelvin = []
Mass_flux_ratio = []
for output in outputs:
    dic = {}
    Pin = output.split('Pin =')[1].split('PSIA')[0].strip()
    O_F = output.split('O/F=')[1].split('%FUEL')[0].strip()
    Temp = output.split('T, K')[1].split('RHO')[0].strip().split()[0]
    flux = output.split('M, (1/n)')[1].split('(dLV/dLP)t')[0].strip().split()[0]
    Isp = output.split('Isp, M/SEC')[1].split('MOLE')[0].strip().split()[1]
    #dic['Pin'] = float(Pin)
    #dic['O_F'] = float(O_F)
    #dic['Isp'] = float(Isp)/9.
    Of_ratio.append(float(O_F))
    Imp.append(float(Isp)/9.81)
    Kelvin.append(float(Temp))
```

```
Mass_flux_ratio.append(float(Temp)/float(flux))

#dic['Temp'] = float(Temp)

df1 = pd.DataFrame(dic, index=[0])
df = pd.concat([df, df1], ignore_index=True)

#Pins = list(df['Pin'].unique())
#colors = ['o-r', 'o-b', 'o-g', 'o-c', 'o-m', 'o-y', 'o-k', 'o-r', 'o-
b', 'o-g', 'o-c', 'o-m', 'o-y', 'o-k']
#cnt = 0

#for Pin in Pins:
    #color = colors[cnt]
    #val = df[df['Pin']==Pin]
    #plt.plot(val['O_F'],val['Isp'],color)
    #plt.plot(val['O_F'],val['Temp'],color)
    #cnt += 1

#plt.legend([str(Pin)+(psia) for Pin in Pins])
#plt.xlabel('O/F ratio')
#plt.ylabel('Isp')
#plt.show()

fig, axs = plt.subplots(2)
fig.suptitle(f'{fuel_name} plus gas oxygen')
axs[0].plot(0f_ratio,Kelvin)
axs[0].set(ylabel='Temp(K)')
```

```
axs[0].set_title('Temperature against oxodizer-fuel ratio')
axs[1].plot(0f_ratio,Imp)
axs[1].set(ylabel='Isp(s)')
axs[1].set_title('Temperature against oxodizer-fuel ratio')
annot_max(np.array(0f_ratio),np.array(Kelvin))

#plt.plot(0f_ratio,Mass_flux_ratio) to plot ratio of heat to molar mass

plt.show()
```

C.2 Nozzle sizing code-Matlab code

```
%Chemistry
% Ethanol GOX

%Ddesign Point
Mftot = 0.71254 %kg/s
OFratio = 1.5
Pc = 2*10^6 %Pa
Pe = 101800 %Pa
%Characteristic length
Lc = 1.43%m

%From NASA CEA
Tc = 3232.42 %K

%propellants molar mass
```

M = 22.035 %kg/kmol

Gamma = 1.2032

%From universal gas constant

R = 414.66

%Ry

Ry = 8314*Gamma

%Throat area

At = (Mftot/Pc)*sqrt(Tc*R/Gamma)*(1+(Gamma -1)/2)^((Gamma+1)/(2*(Gamma -1)))

%Throat diameter

Dt = 2 * sqrt(At/3.142)

%Exit Mach Number

Me = sqrt((2*((Pe/Pc)^-(((Gamma -1)/Gamma))-1))/(Gamma-1))

%Let Ar be the ratio Ae/At

Ar = (1/Me)*((2/(Gamma+1))*(1+(((Gamma-1)/2))*Me^2))^((Gamma+1)/(2*(Gamma-1)))

%Area of exit

Ae = At * Ar

%Exit area diameter

De = 2 * sqrt(Ae/3.142)

%Exit velocity

Ue = sqrt(2 * Ry/(Gamma-1)*(Tc/M) * (1 - (Pe/Pc)^((Gamma-1)/Gamma)))

%Specific Impulse

I_{sp} = U_e/9.8

%Thrust

F = M_{ftot} * U_e

%Chamber volume

V_c = A_t * L_c

A_c = A_t * (8*((D_t*100)^-0.6) + 1.25)

%Actual chamber length

L_{ch} = V_c / A_c

D_c = 2 * sqrt(A_c/3.142)

%Ending point

%L_c = 0.17

%D_c = 0.054

%Nozzle expanding at 15 degrees

theta_n = 15

L_n = (D_e-D_t)/(2*tand(theta_n))

Appendix D

Design reference tables, charts

TABLE 14.2a. Dimensions and Physical Characteristics of Copper Tube: Type K

Nominal or standard size, inches	Nominal dimensions, inches			Calculated values (based on nominal dimensions)				Volume of tube, per linear ft.	
	Outside diameter	Inside diameter	Wall thickness	Cross sectional area of bore, sq. inches	Weight of tube only, pounds per linear ft.	Weight of tube & water, pounds per linear ft.	Cu ft.	Gal.	
								Cu ft.	Gal.
1/4	.375	.305	.035	.073	.145	.177	.00051	.00379	
3/8	.500	.402	.049	.127	.269	.324	.00088	.00660	
1/2	.625	.527	.049	.218	.344	.438	.00151	.0113	
5/8	.750	.652	.049	.334	.418	.562	.00232	.0174	
3/4	.875	.745	.065	.436	.641	.829	.00303	.0227	
1	1.125	.995	.065	.778	.839	1.18	.00540	.0404	
1 1/4	1.375	1.245	.065	1.22	1.04	1.57	.00847	.0634	
1 1/2	1.625	1.481	.072	1.72	1.36	2.10	.0119	.0894	
2	2.125	1.959	.083	3.01	2.06	3.36	.0209	.156	
2 1/2	2.625	2.435	.095	4.66	2.93	4.94	.0324	.242	
3	3.125	2.907	.109	6.64	4.00	6.87	.0461	.345	
3 1/2	3.625	3.385	.120	9.00	5.12	9.01	.0625	.468	
4	4.125	3.857	.134	11.7	6.51	11.6	.0813	.608	
5	5.125	4.805	.160	18.1	9.67	17.5	.126	.940	
6	6.125	5.741	.192	25.9	13.9	25.1	.180	1.35	
8	8.125	7.583	.271	45.2	25.9	45.4	.314	2.35	
10	10.125	9.449	.338	70.1	40.3	70.6	.487	3.64	
12	12.125	11.315	.405	101	57.8	101	.701	5.25	